This is to certify that the

thesis entitled

A MODELING STUDY OF PLUG MUFFLER PERFORMANCE

presented by

KIT LEUNG YAM

has been accepted towards fulfillment
of the requirements for

M.S. degree in Ch. E.

K Jayaraman
Major professor

Date 11/14/80

A MODELING STUDY OF PLUG MUFFLER PERFORMANCE

By

Kit Leung Yam

A THESIS

Submitted to
Michigan State University
in partial fulfillment of the requirements
for the degree of

MASTER OF SCIENCE

Department of Chemical Engineering

1980

ABSTRACT

A MODELING STUDY OF PLUG MUFFLER PERFORMANCE

By

Kit Leung Yam

A new approach has been described for solving problems of plane acoustic propagation in mufflers with partitioned, perforated tubes with mean flow, by decoupling the governing differential equations. This approach leads to compact and exact expressions for the matrix parameters of crossflow elements without any concern for convergence of infinite series or segmental analysis employed in other studies. The predicted transmission loss curves agree remarkably well with experimental results in zero mean flow, and for mean flow Mach numbers at least up to .16. Various muffler configurations can be modeled easily by applying the appropriate boundary conditions. The resonance frequencies of a plug muffler with no mean flow are seen to coincide with resonance frequencies of crossflow elements, which in turn may be correlated very simply and accurately with the dimensionless group $(\psi\ell)^2$ defined in this work. This correlation bears out observed trends with variation of geometric parameters.

Dedication

To My Parents and Alice

ACKNOWLEDGEMENTS

I would like to express my deepest appreciation to Dr. K. Jayaraman, my academic advisor, for his constant encouragement and direction. I would also like to extend my thanks to the Department of Chemical Engineering at Michigan State University and the Nelson Industries at Stoughton, Wisconsin, for their very kind financial assistance during the course of my Master program.

CHA

I

II

I

V

V

REF

APP

TABLE CONTENTS

CHAPTER I

INTRODUCTION

Mufflers for a variety of applications involve perforated tubes encased in concentric chambers. Despite their popular usage, the design of these mufflers is largely empirical. As restrictions on noise control, exhaust system size and manufacturing cost become tightened, the time consuming trial-and-error approach is found to be inefficient and inadequate. There is a strong desire for a model which can provide better understandings on the performance of such mufflers in order to develop more sophisticated and effective designs.

Sullivan [1] has derived a closed form analytical solution for the differential equations describing the plane wave motion in the cavity and in the center tube of an unpartitioned concentric resonator. Jayaraman [2] has shown that the performance of such resonators, in the absence of mean flow, can be analyzed more clearly by decoupling the differential equations using two transformed variables, one of them being the radial particle velocity through the perforated interface.

Sullivan [3] has further shown that mufflers with plugged perforated tubes in a chamber may be treated as a combination of two crossflow elements with different terminations on the two ducts involved in each crossflow element. He has suggested that the transmission matrix parameters describing plane wave propagation in each element be

com

sep

bra

Sul

use

obt

ver

the

cer

the

tia

tho

Ja

ut

lu

in

pe

ma

te

ef

0.

tw

nu

te

computed by lumping the perforate impedance into several branches separating rigid walled segments. Each of these segments and associated branches would be described by a 4 x 4 transmission matrix; for Sullivan's example of a tube with 3.9 percent porosity, 15 segments were used so that 30 such matrices were multiplied at each frequency to obtain, after applying the appropriate termination conditions, the conventional 2 x 2 transmission matrix of a crossflow element.

The difference between the unpartitioned concentric resonator and the plug muffler lies, insofar as mathematical representation is concerned, in the more complicated assortment of boundary conditions for the crossflow elements which constitute the plug muffler. The differential equations describing plane wave propagation in the two ducts are the same in both cases. In this work, a treatment similar to that of Jayaraman's analysis is used to decouple the one-dimensional, distributed model as described by Sullivan. This analysis leads, without any lumping, into two "straight pipe" equations for transformed variables including the effect of convection due to mean flow as well as complex perforate impedance. The resulting expressions for the transmission matrix parameters of the crossflow element, incorporating any set of terminations, are exact and may be used to explore more directly the effect of parameter variations on transmission loss curves.

For typical exhaust systems, mean flow Mach numbers ranging up to 0.3 are representative. The effect of mean flow is to be discussed in two aspects: (1) computing perforate resistance for mean flow Mach number and (2) analyzing the differential equations with "convective terms" present. An assumption, which shall be shown to be required by

the decoupling approach, is that the tube and the chamber of the concentric component have the same mean flow. This condition is normally not satisfied in practice because the cross-sectional areas of the tube and the chamber are usually unequal. However, this assumption does not seem to be restrictive for mean flow Mach numbers at least up to .16. Moreover, for much higher mean flow, an average Mach number for the tube and the chamber may be used in this model.

Various muffler configurations can be modeled easily by applying the appropriate boundary conditions to the decoupling model. The muffler configurations discussed here include plug mufflers, diffusers and mufflers with more than one plug. Transmission loss curves computed as a function of frequency are compared with curves obtained from experiments when available. The locations and widths of resonance peaks are discussed for each configuration. The contribution of each crossflow element to the combined muffler is also examined closely.

Finally, a simple relation between the resonance peak locations of a crossflow element and its geometric parameters is obtained. This relation allows very accurate resonance peak locations prediction for crossflow elements in the absence of mean flow.

CHAPTER II

MODEL EQUATIONS FOR PERFORATED TUBE RESONATORS

The differential equations describing plane wave propagation in the two duct configuration [see Figure 1] presented here are proposed by Sullivan and Crocker [1]. The principal assumptions used in the formulation of these equations are as follow:

(1) Negligible spatial variations of acoustic pressure and related density over any cross-section of either the tube or the cavity.

(2) Fluctuating pressure and density are small compared to the mean values.

(3) Gradients of mean flow and temperature are neglected.

(4) The only losses in the system are caused by the resistance at the interface between the tube and the cavity.

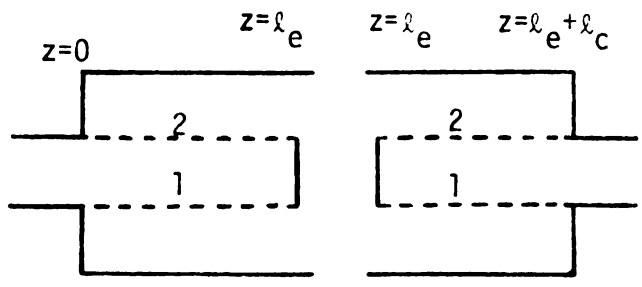

Figure 1. Configuration of Crossflow Elements.

be wr

for t

for t

time-

w_2',

velo

radi

ing

freq

and

$c_c c_\zeta$

we ob

The equation of mass conservation and momentum conservation may be written as

$$W_1 \frac{\partial \rho_1^{|}}{\partial z} + \rho_o \frac{\partial w_1^{|}}{\partial z} + \frac{4}{d_1} \rho_o u^{|} = - \frac{\partial \rho_1^{|}}{\partial t} \tag{2.1}$$

$$\rho_o \left(\frac{\partial}{\partial t} + W_1 \frac{\partial}{\partial z}\right) w_1^{|} = - \frac{\partial p_1^{|}}{\partial z} \tag{2.2}$$

for the inner tube (duct 1) of diameter d_1; and

$$W_2 \frac{\partial \rho_2^{|}}{\partial z} + \rho_o \frac{\partial w_2^{|}}{\partial z} - \frac{4d_1}{(d_2^2 - d_1^2)} \rho_o u^{|} = - \frac{\partial \rho_2^{|}}{\partial t} \tag{2.3}$$

$$\rho_o \left(\frac{\partial}{\partial t} + W_2 \frac{\partial}{\partial z}\right) w_2^{|} = - \frac{\partial p_2^{|}}{\partial z} \tag{2.4}$$

for the cavity (duct 2) of diameter d_2. Here ρ_o, W_1 and W_2 denote the time-mean density and the time-mean axial flow velocities while $w_1^{|}$, $w_2^{|}$, $\rho_1^{|}$, $\rho_2^{|}$ and $p_1^{|}$, $p_2^{|}$ denote the fluctuations in axial particle velocity, density and pressure in the two ducts; $u^{|}$ is the fluctuating radial particle velocity in the perforations; setting $p^{|} = \rho^{|} c^2$, replacing all fluctuating quantities by their complex amplitudes for a given frequency ω according to

$$p^{|} = p(z)\, e^{i\omega t} \; ; \; u^{|} = u(z) e^{i\omega t} \text{ etc.} \quad , \quad i \equiv \sqrt{-1}$$

and relating $u(z)$ to $p_1(z)$ and $p_2(z)$ by the uniform perforate impedance $\rho_o c \zeta$

$$u(z) = \frac{p_1(z) - p_2(z)}{\rho_o c \zeta} \tag{2.5}$$

we obtain the coupled differential equations

$$\left[\frac{d^2}{dz} - \frac{iM_1}{1-M_1^2}\left(\frac{k_a^2+k^2}{k}\right)\frac{d}{dz} + \frac{k_a^2}{1-M_1^2}\right] p_1(z) =$$

$$- \left[\frac{iM_1}{1-M_1^2}\left(\frac{k_a^2-k^2}{k}\right)\frac{d}{dz} - \frac{k_a^2-k^2}{1-M_1^2}\right] p_2(z) \qquad (2.6)$$

for the center tube and

$$\left[\frac{d^2}{dz^2} - \frac{iM_2}{1-M_2^2}\left(\frac{k_b^2+k^2}{k}\right)\frac{d}{dz} + \frac{k_b^2}{1-M_2^2}\right] p_2(z)$$

$$= - \left[\frac{iM}{1-M^2}\left(\frac{k_b^2-k^2}{k}\right)\frac{d}{dz} - \frac{k_b^2-k^2}{1-M^2}\right] p_1(z) \text{ for the cavity} \qquad (2.7)$$

where $k \equiv \omega/c \quad M_1 \equiv \frac{W_1}{c} \quad M_2 \equiv \frac{W_2}{c}$

$$k_a^2 \equiv k^2 - i\frac{4k}{d_1\zeta} \quad k_b^2 \equiv k^2 - i\frac{4d_1k}{(d_2^2-d_1^2)\zeta} \qquad (2.8)$$

and $c \equiv$ speed of sound.

A closed form solution of the above differential equations for concentric resonators has been obtained by Sullivan [1] using an eigenfunction expansion method. In his solution, it is assumed that there was mean flow in the tube but not in the cavity.

CHAPTER III

SOLUTION TO MODEL EQUATIONS

In this chapter, a decoupling approach will be used to solve the model equations with mean flow included both in the tube and in the chamber. For simplicity, temperature, porosity, mean flow and impedance of perforation are assumed to be uniform along the crossflow elements. This approach allows a clear and direct parameter analysis on the transmission loss curves to be studied.

3.1 Decoupling Analysis

Two transformed variables Γ_1 and Γ_2 (which are combinations of p_1 and p_2) are used to decouple the differential equations given in Chapter II into propagation equations similar to equations for the straight pipe. Equations (2.6 and 2.7) may be rearranged to a compact matrix form

$$\underbrace{\begin{bmatrix} D^2 - \alpha_1 D + \alpha_2 & \alpha_3 D - \alpha_4 \\ \alpha_5 D - \alpha_6 & D^2 - \alpha_7 D + \alpha_8 \end{bmatrix}}_{\underline{A}} \begin{bmatrix} P_1(z) \\ P_2(z) \end{bmatrix} = 0 \qquad (3.1)$$

where $D \equiv d/dz$ and the α's may be identified by comparison with equations (2.6) and (2.7).

$$\alpha_1 \equiv \frac{iM_1}{1-M_1^2}\left(\frac{k_a^2+k^2}{k}\right) \qquad \alpha_2 \equiv \frac{k_a^2}{1-M_1^2}$$

$$\alpha_3 \equiv \frac{iM_1}{1-M_1^2}\left(\frac{k_a^2-k^2}{k}\right) \qquad \alpha_4 \equiv \frac{k_a^2-k^2}{1-M_1^2}$$

$$\alpha_5 \equiv \frac{iM_2}{1-M_2^2}\left(\frac{k_b^2-k^2}{k}\right) \qquad \alpha_6 \equiv \frac{k_b^2-k^2}{1-M_2^2}$$

$$\alpha_7 \equiv \frac{iM_2}{1-M_2^2}\left(\frac{k_b^2+k^2}{k}\right) \qquad \alpha_8 \equiv \frac{k_b^2}{1-M_2^2} \tag{3.2}$$

The operator matrix, $\underline{\underline{A}}$, in (3.1) may be diagonalized by assuming that it is similar to a diagonal matrix of the form

$$\underline{\underline{\Lambda}} \equiv \begin{bmatrix} \gamma_1 D^2 - \gamma_2 D + \gamma_3 & 0 \\ 0 & \gamma_4 D^2 - \gamma_5 D + \gamma_6 \end{bmatrix} \tag{3.3}$$

By matching terms in the characteristic polynomials of A and $\underline{\underline{\Lambda}}$, the following equations

$$\gamma_1 + \gamma_4 = 2 \tag{3.4}$$

$$\gamma_2 + \gamma_5 = \alpha_1 + \alpha_7 \tag{3.5}$$

$$\gamma_3 + \gamma_5 = \alpha_2 + \alpha_8 \tag{3.6}$$

$$\gamma_1\gamma_4 = 1 \tag{3.7}$$

$$\gamma_1\gamma_5 + \gamma_2\gamma_4 = \alpha_1 + \alpha_7 \tag{3.8}$$

$$\gamma_1\gamma_6 + \gamma_2\gamma_5 + \gamma_3\gamma_4 = \alpha_2 + \alpha_8 + \alpha_1\alpha_7 - \alpha_3\alpha_5 \tag{3.9}$$

$$\gamma_2\gamma_6 + \gamma_3\gamma_5 = \alpha_1\alpha_8 + \alpha_2\alpha_7 - \alpha_3\alpha_6 - \alpha_4\alpha_5 \tag{3.10}$$

$$\gamma_3\alpha_6 = \alpha_2\alpha_8 - \alpha_4\alpha_6 \tag{3.11}$$

must all be satisfied in order to obtain a consistent solution. Solving equations (3.4) and (3.7), $\gamma_1 = \gamma_4 = 1$. Therefore equation (3.8) can be reduced to equation (3.5), and equation (3.9) can be simplified as

$$\gamma_2\gamma_5 = \alpha_1\alpha_7 - \alpha_3\alpha_5 \tag{3.12}$$

There remains four unknowns (γ_2, γ_3, γ_5 and γ_6) and five equations ((3.5), (3.6), (3.10), (3.11), (3.12)). By solving equations (3.5) and (3.12),

$$\gamma_5 = \frac{(\alpha_1 + \alpha_7) \pm \sqrt{(\alpha_1 + \alpha_7)^2 - 4(\alpha_1\alpha_7 - \alpha_3\alpha_5)}}{2} \tag{3.13}$$

and arbitrary pick

$$\gamma_5 = \frac{(\alpha_1 + \alpha_7) + \sqrt{(\alpha_1 + \alpha_7)^2 - 4(\alpha_1\alpha_7 - \alpha_3\alpha_5)}}{2} \tag{3.14}$$

such that

$$\gamma_2 = \frac{(\alpha_1 + \alpha_7) - \sqrt{(\alpha_1 + \alpha_7)^2 - 4(\alpha_1\alpha_7 - \alpha_3\alpha_5)}}{2} \tag{3.15}$$

Similarly, solving equations (3.6) and (3.11)

$$\gamma_6 = \frac{(\alpha_2 + \alpha_8) \pm \sqrt{(\alpha_2 + \alpha_8)^2 - 4(\alpha_2\alpha_8 - \alpha_4\alpha_6)}}{2} \tag{3.16}$$

and again arbitrary pick

$$\gamma_6 = \frac{(\alpha_2 + \alpha_8) + \sqrt{(\alpha_2 + \alpha_8)^2 - 4(\alpha_2\alpha_8 - \alpha_4\alpha_6)}}{2} \tag{3.17}$$

such that

$$\gamma_3 = \frac{(\alpha_2 + \alpha_8) - \sqrt{(\alpha_2 + \alpha_8)^2 - 4(\alpha_2\alpha_8 - \alpha_4\alpha_6)}}{2} \tag{3.18}$$

Equations (3.14). (3.15), (3.17) and (3.18) compose a set of consistent solutions only if the remaining equation (3.10) is also satisfied. Equation (3.10) is satisfied only if the mean flow Mach numbers in the two ducts are assumed to be identical (i.e., $M_1 = M_2 = M$). Note that this assumption cannot be eliminated even if γ_2 and γ_3 take the positive roots of the discriminates in equations (3.13) and (3.16), respectively. After substituting the α's by equation (3.2), the γ's are given by

$$\gamma_1 = 1 \qquad\qquad \gamma_1 = 1$$

$$\gamma_2 = \frac{iM}{1-M^2}\left(\frac{k_a^2 + k_b^2}{k}\right) \qquad\qquad \gamma_5 = \frac{2iM}{1-M^2}\,k \tag{3.19}$$

$$\gamma_3 = \frac{1}{1-M^2}\left(k_a^2 + k_b^2 - k^2\right) \qquad\qquad \gamma_6 = \frac{k^2}{1-M^2}$$

so the decoupled equations are

$$\left(D^2 - \frac{iM}{1-M^2}\,\frac{(k_1^2 + k^2)}{k}\,D + \frac{k_1^2}{1-M^2}\right)\,\Gamma_1 = 0 \tag{3.20}$$

$$\left(D^2 - \frac{2iM}{1-M^2}\,kD + \frac{k^2}{1-M^2}\right)\,\Gamma_2 = 0 \tag{3.21}$$

where $k_1^2 \equiv k^2 - \frac{i\,4\,k}{d_1\zeta}\left(\frac{1}{1-r^2}\right)$; $r \equiv d_1/d_2$ (3.22)

Following a similar analysis to Jayaraman's earlier work, a new pair of pressures Γ_1 and Γ_2, which are combinations of P_1 and P_2 , are defined by

$$\begin{bmatrix} P_1 \\ P_2 \end{bmatrix} = \underline{\underline{S}} \begin{bmatrix} \Gamma_1 \\ \Gamma_2 \end{bmatrix} \tag{3.23}$$

where $\underline{\underline{S}}$ is the matrix of eigenvecroea of $\underline{\underline{A}}$ in equation (3.1). The eigenvalues of $\underline{\underline{A}}$ are given as the diagonal elements in equation (3.3), where the γ's are given in equation (3.19).

For the eigenvalue $\lambda_1 = \gamma_1 D^2 - \gamma_2 D + \gamma_3$,

$$\underline{\underline{A}} - \lambda_1 \underline{\underline{I}} = \begin{bmatrix} (\gamma_2-\alpha_1)\, D + (\alpha_2 - \gamma_3) & \alpha_3 D - \alpha_4 \\ \alpha_5 D - \alpha_6 & (\gamma_2 - \alpha_7)\, D + (\alpha_8 - \gamma_3) \end{bmatrix}$$

$$= \begin{bmatrix} \frac{iM}{1-M^2}\left(\frac{k_b^2-k^2}{k}\right) D + (k^2-k_b^2) & \frac{iM}{1-M^2}\left(\frac{k_a^2-k^2}{k}\right) D + (k^2-k_a^2) \\ \frac{iM}{1-M^2}\left(\frac{k_b^2-k^2}{k}\right) D + (k^2-k_b^2) & \frac{iM}{1-M^2}\left(\frac{k_a^2-k^2}{k}\right) D + (k^2-k_a^2) \end{bmatrix}$$

$$= \left[\frac{iM}{1-M^2}\left(\frac{k_b^2-k^2}{k}\right) D + (k^2-k_b^2)\right] \begin{bmatrix} 1 & \frac{1-r^2}{r^2} \\ 1 & \frac{1-r^2}{r^2} \end{bmatrix} \qquad (3.24)$$

so the eigen-solution is given by

$$P_1 + \frac{1-r^2}{r^2} P_2 = 0$$

Setting $P_1 = 1$, the eigenvector for λ_1 is thus

$$\begin{bmatrix} 1 \\ \frac{r^2}{r^2-1} \end{bmatrix}$$

Similarly, the eigenvector for $\lambda_2 = \gamma_4 D^2 - \gamma_5 D + \gamma_6$ can be found to be $\begin{bmatrix} 1 \\ 1 \end{bmatrix}$ Therefore the eigenvectors matrice is

and

As a ch

cation.

T

and p_2.

The ne

equati

Furthe

throug

[so th

equati

as

$$\underline{\underline{S}} = \begin{bmatrix} 1 & 1 \\ \frac{r^2}{r^2-1} & 1 \end{bmatrix} \tag{3.25}$$

and

$$\underline{\underline{S}}^{-1} = \begin{bmatrix} 1-r^2 & r^2-1 \\ r^2 & 1-r^2 \end{bmatrix} \tag{3.26}$$

As a check, the relation $\underline{\underline{S}}^{-} \underline{\underline{A}}\ \underline{\underline{S}} = \underline{\underline{\Lambda}}$ can be shown by direct multiplication.

The two transformed variables can now be expressed in terms of p_1 and p_2.

$$\Gamma_1 = (1-r^2)\ (p_1 - p_2) \tag{3.27}$$

$$\Gamma_2 = r^2\ \ (p_1\ \ - p_2) + p_2 \tag{3.28}$$

The new "pressures" Γ_1 and Γ_2 follow equations similar to the classic equation for plane wave propagation with mean flow in a straight pipe. Further, $\Gamma_1\ (z)$ is directly related to the fluctuating radial velocity through the perforations--

$$\Gamma_1\ (z) = (1-r^2)\ \ \rho_o c\zeta\ \ u(z); \tag{3.29}$$

[so the radial particle velocity propagates with wavenumber k_1 given by equation (3.22), in the absence of mean flow].

The general solutions to equations (3.20) and (3.21) are obtained as

$$\Gamma_1\ (z) = \Gamma_1^{+}\ e^{-i\phi_2 z} + \Gamma_1^{-}\ e^{i\phi_2 z} \tag{3.30}$$

$$\Gamma_1\ (z) = \Gamma_2^{+}\ e^{-i\phi_3 z} + \Gamma_2^{-}\ e^{i\phi_4 z} \tag{3.31}$$

where

We n

ati

3.2

ma

ar

F

t

t

where

$$\left.\begin{aligned}
\Phi_1 &= \frac{M}{2(1-M^2)}\left[-\left(\frac{k_1^2+k^2}{k}\right) + \sqrt{\frac{4k_1^2}{M} - 4k_1^2 + \left(\frac{k_1^2+k}{k}\right)^2}\right] \\
\phi_2 &= \frac{M}{2(1-M^2)}\left[\left(\frac{k_1^2+k^2}{k}\right) + \sqrt{\frac{4k_1^2}{M^2} - 4k_1^2 + \left(\frac{k_1^2+k^2}{k}\right)^2}\right] \\
\phi_3 &= \frac{k}{1+M} \quad ; \quad \phi_4 = \frac{k}{1-M}
\end{aligned}\right\} \tag{3.32}$$

We may now incorporate any set of terminations on the two duct configuration to obtain the matrix parameters.

3.2 Terminations and Matrix Parameters

To take account of the boundary conditions in the two ducts, we may use the relations

$$p_1(z) = \Gamma_1(z) + \Gamma_2(z) \tag{3.33}$$

and

$$p_2(z) = \frac{r^2}{r^2-1}\,\Gamma_1(z) + \Gamma_2(z) \tag{3.34}$$

For example in the case of the crossflow expansion chamber, with rigid terminations at $z = 0$ in the cavity and at $z = \ell$ in the center tube, the boundary conditions

$$\frac{dp_1}{dz}(\ell) = 0 \text{ and } \frac{dp_2}{dz}(0) = 0 \tag{3.35}$$

may be combined with equations (3.33), (3.34), (3.30), and (3.31) to obtain

$$-i\phi_1\Gamma_1^{+}e^{-i\phi_1\ell} + i\phi_2\Gamma_1^{-}e^{i\phi_2\ell} - i\phi_3\Gamma_2^{+}e^{-i\phi_3\ell} + i\phi_4\Gamma_2^{-}e^{i\phi_4\ell} = 0 \tag{3.36}$$

$$(-i\phi_1\Gamma_1^{+} + i\phi_2\Gamma_1^{-})\,\frac{r^2}{r^2-1} - i\phi_3\Gamma_2^{+} + i\phi_4\Gamma_2^{-} = 0 \tag{3.37}$$

which allow elimination of Γ_2^+ and Γ_2^- from the relations for p_1 and p_2. Next, the equations

$$(ik + M\frac{d}{dz})\, w_j(z) = -\frac{1}{\rho_o}\frac{d}{dz}\, p_j(z) \quad j = 1,2 \tag{3.38}$$

may be used to obtain expressions for $w_j(z)$ in terms of Γ_1^+ and Γ_1^-. Finally we may write

$$\left.\begin{aligned} p_1(0) &= \tau_1\Gamma_1^+ + \tau_2\Gamma_1^- \\ \rho_o c w(0) &= \tau_3\Gamma_1^+ + \tau_4\Gamma_1^- \\ p_2(\ell) &= \tau_5\Gamma_1^+ + \tau_6\Gamma_1^- \\ \rho_o c w_2(\ell) &= \tau_7\Gamma_1^+ + \tau_8\Gamma_1^- \end{aligned}\right\} \tag{3.39}$$

where the $\{\tau_j\}$ involving only M, k, k_1 and ℓ are given by expressions noted in the Appendix.

Γ_1^+ and Γ_1^- may be eliminated from (3.39) to obtain the transmission matric

$$\begin{bmatrix} p_1(0) \\ \rho_o c w_1(0) \end{bmatrix} = \begin{bmatrix} T_{Ae} & T_{Be} \\ T_{Ce} & T_{De} \end{bmatrix} \begin{bmatrix} P_2(\ell) \\ \rho_o c w_2(\ell) \end{bmatrix} \tag{3.40}$$

where

$$\left.\begin{aligned} T_{Ae} &= \frac{1}{F}(\tau_1\tau_8 - \tau_2\tau_7) \\ T_{Be} &= \frac{1}{F}(\tau_2\tau_5 - \tau_1\tau_6) \\ T_{Ce} &= \frac{1}{F}(\tau_3\tau_8 - \tau_4\tau_7) \\ T_{De} &= \frac{1}{F}(\tau_4\tau_5 - \tau_3\tau_6) \\ F &\equiv (\tau_5\tau_8 - \tau_6\tau_7) \end{aligned}\right\} \tag{3.41}$$

These expressions represent the exact solution of the two coupled differential equations (2.6) and (2.7) subject to the boundary conditions of a crossflow expansion chamber. The transmission loss at any frequency may be computed from the matric parameters by

$$TL = 10 \log_{10} \{ \frac{A_i}{A_o} \left(\frac{1+M_i}{1+M_o}\right)^2 \left|\frac{T_A+T_B+T_C+T_D}{2}\right|^2 \} \qquad (3.42)$$

where A_i and A_o are inlet and outlet areas of cross section for the crossflow elements; M_i and M_o refer to incoming and outgoing mean flow Mach numbers. Similar analysis for a crossflow contraction chamber with boundary conditions

$$\frac{dp_1}{dz}(0) = 0 \quad , \quad \frac{dp_2}{dz}(\ell) = 0 \qquad (3.43)$$

yields the same expressions as in (3.41) for the matric parameters but with slight modifications in the $\{\tau_j\}$ as noted in the Appendix.

CHAPTER IV

MODEL SIMULATIONS ON TL CURVES FOR PLUG MUFFLERS WITH NO MEAN FLOW

Effects of varying plug location and porosity of plug mufflers, with no mean flow, on transmission loss curves are examined in this chapter. The impedance measurements used here are obtained from the works by Jayaraman [2] and Sullivan [3].

4.1 Theoretical Expression for Matrix Parameters of Plug Mufflers

A simpler approach compared to that described in the last chapter can be used here to decouple the differential equations describing the plane wave motion of crossflow elements. For the mean flow Mach number M=0, equations (2.6) and 2.7) can be simplified to

$$\text{Center tube} \quad \frac{d^2p_1(z)}{dz^2} + k_a^2 p_1(z) = (k_a^2 - k^2)\, p_2(z) \tag{4.1}$$

$$\text{Chamber} \quad \frac{d^2p_2(z)}{dz^2} + k_b^2\, p_2(z) = (k_b^2 - k^2)\, p_1(z) \tag{4.2}$$

The two equations may be rewritten as:

$$\frac{d^2}{dz^2}\begin{bmatrix} p_1 \\ p_2 \end{bmatrix} = \underbrace{\begin{bmatrix} -k_a^2 & k_a^2 - k^2 \\ k_b^2 - k^2 & -k_b^2 \end{bmatrix}}_{\underline{A}'} \begin{bmatrix} p_1 \\ p_2 \end{bmatrix} \tag{4.3}$$

Again, a formal eigenvector analysis yields the decoupled equations

$$\frac{d^2\Gamma_1}{dz^2} + k_1^2\Gamma_1 = 0 \tag{4.4}$$

$$\frac{d^2\Gamma_2}{dz^2} + k^2\Gamma_2 = 0 \tag{4.5}$$

Γ_1 and Γ_2 are the transformed variable which are related to p_1 and p_2 by equations (3.26) and (3.27). Referring back to Figure 1, on page 4, denoting Γ_1, Γ_2 at $z = \ell_e$ by Γ_{12},Γ_{22}, and at $z = \ell_e + \ell_c$ by Γ_{13},Γ_{33}, we obtain first from equations (4.4) and then (4.5).

$$\begin{bmatrix} \Gamma_{12} \\ \frac{d\Gamma_{12}}{dz} \\ \Gamma_{22} \\ \frac{d\Gamma_{22}}{dz} \end{bmatrix} \underbrace{\begin{bmatrix} \cos k_1\ell & \frac{-\sin k_1\ell}{k} & 0 & 0 \\ k_1 \sin k_1\ell & \cos k_1\ell & 0 & 0 \\ 0 & 0 & \cos k\ell & \frac{-\sin k\ell}{k} \\ 0 & 0 & k\sin k\ell & \cos k\ell \end{bmatrix}}_{\underline{\underline{I}}} \begin{bmatrix} \Gamma_{13} \\ \frac{d\Gamma_{13}}{dz} \\ \Gamma_{23} \\ \frac{d\Gamma_{23}}{dz} \end{bmatrix} \tag{4.6}$$

This occurs because the decoupled equations for Γ_1 and Γ_2 are mathematically identical with the straight pipe equations for plane wave propagation.

Going back to pressures

$$\begin{pmatrix} p_{12} \\ \frac{dp_{12}}{dz} \\ p_{22} \\ \frac{dp_{22}}{dz} \end{pmatrix} = \underline{\underline{R}}\,\underline{\underline{I}}\,\underline{\underline{R}}^{-1} \begin{pmatrix} p_{13} \\ \frac{dp_{13}}{dz} \\ p_{23} \\ \frac{dp_{23}}{dz} \end{pmatrix} \tag{4.7}$$

where $\underline{\underline{R}}$ is the matrix of eigenvectors of $\underline{\underline{A'}}$.

$$\underline{\underline{B}} = \begin{pmatrix} 1 & 0 & 1 & 0 \\ 0 & 1 & 0 & 1 \\ \frac{1}{1-1/r^2} & 0 & 1 & 0 \\ 0 & \frac{1}{1-1/r^2} & 0 & 1 \end{pmatrix} \qquad r \equiv D_1/D_2 \qquad (4.8)$$

$$\underline{\underline{B}}^{-1} = \begin{pmatrix} 1-r^2 & 0 & -1+r^2 & 0 \\ 0 & 1-r^2 & 0 & -1+r^2 \\ r^2 & 0 & 1-r^2 & 0 \\ 0 & r^2 & 0 & 1-r^2 \end{pmatrix} \qquad (4.9)$$

The boundary conditions for the crossflow contraction chamber are

$$\frac{dp_{12}}{dz} = 0, \text{ and } \frac{dp_{23}}{dz} = 0 \qquad (4.10)$$

may be used to eliminate from equation (4.7) p_{12}, $\frac{dp_{12}}{dz}$ from the left and p_{23}, $\frac{dp_{23}}{dz}$ from the right yielding a 2 x 2 matrix. In addition, knowing that the amplitudes of pressure, p, and particle velocity, v, are related by

$$\frac{1}{k}\frac{dp}{dz} = -i\rho cv \qquad (4.11)$$

on either side, we obtain the transmission matrix $\underline{\underline{T}}_c$ for the crossflow contraction chamber in the relation

$$\begin{pmatrix} p_{22} \\ \rho c v_{22} \end{pmatrix} = \begin{pmatrix} T_{Ac} & T_{Bc} \\ T_{Cc} & T_{Dc} \end{pmatrix} \begin{pmatrix} p_{13} \\ \rho c v_{13} \end{pmatrix} \qquad (4.12)$$

$$\underline{\underline{T}}_c$$

where

$$T_{AC} = [r^2F_1F_4/(r^2-1) - F_2F_3]/(F_4-F_3)$$

$$T_{BC} = ik[r^2(2-2F_1F_2 - F_4F_5 - F_3F_6) - F_1F_2/(r^2-1)]/(F_4-F_3)$$

$$T_{CC} = F_3F_4/[ik(1-r^2)\ (F_4-F_3)]$$

$$T_{DC} = [r^2F_2F_3/(r^2-1) - F_1F_4]/(F_4- F_3) \qquad (4.13)$$

$$F_1 = \cos k_1 l \qquad F_4 = k \sin kl$$

$$F_2 = \cos kl \qquad F_5 = \frac{1}{k_1} \sin k_1 l$$

$$F_3 = k_1 \sin k_1 l \qquad F_6 = \frac{1}{k} \sin kl$$

$$r = d_1/d_2 \qquad (4.14)$$

Similarly, denoting p_1, p_2 at $z = 0$ by p_{11}, p_{21} and applying the boundary conditions for the crossflow contraction chamber,

$$\frac{dp_{21}}{dz} = 0 \quad \text{and} \quad \frac{dp_{12}}{dz} = 0 \qquad (4.15)$$

We obtain the transmission matrix T_e for the crossflow expansion chamber in the relation

$$\begin{pmatrix} p_{11} \\ \rho c v_{11} \end{pmatrix} = \underbrace{\begin{pmatrix} T_{Ae} & T_{Be} \\ T_{Ce} & T_{De} \end{pmatrix}}_{\underline{\underline{T}}_e} \begin{pmatrix} p_{22} \\ \rho c v_{22} \end{pmatrix} \qquad (4.16)$$

The matrix parameters for a crossflow expansion element may be obtained from the crossflow contraction transmission parameters of equal chamber length and porosity by the relations

$$\begin{pmatrix} T_{Ae} & T_{Be} \\ T_{Ce} & T_{De} \end{pmatrix} = \frac{1-r^2}{1-r^2} \begin{pmatrix} T_{Dc} & T_{Bc} \\ T_{Cc} & T_{Ac} \end{pmatrix} \tag{4.17}$$

The overall transmission matrix $\underline{\underline{T}}$ of the plug muffler can now be obtained by multiplying the matrices $\underline{\underline{T}}_e$ and $\underline{\underline{T}}_c$.

$$\underline{\underline{T}} = \underline{\underline{T}}_e \underline{\underline{T}}_c = \begin{bmatrix} T_A & T_B \\ T_C & T_D \end{bmatrix} \tag{4.18}$$

The transmission loss TL may be evaluated by equation (3.41) to be

$$TL = 10 \log_{10} \{ \frac{A_i}{A_o} \left| \frac{T_A + T_B + T_C + T_D}{2} \right|^2 \} \tag{4.19}$$

where A_i and A_o are inlet and outlet cross-sectional areas for the cross-flow elements.

For equal chamber length and porosity, the transmission losses TL_e for the crossflow expansion chamber and TL_c for the crossflow contraction chamber is related by

$$TL_e = TL_c \tag{4.20}$$

The transmission matrices derived here are consistent with the transmission matrices obtained from setting M = 0 in equation (3.40). One check on the numbers obtained from the computer is that the determinant of the overall transmission matrix should be unity for mufflers without mean flow.

For completeness we note here that similarly, the following equations may be derived for the concentric unpartitioned resonator in the

absence of mean flow.

$$T_A = \frac{\frac{r^2}{r^2-1} F_2F_3 - F_1F_4}{\frac{r^2}{r^2-1} F_3 - F_4}$$

$$T_B = \frac{ik}{\frac{r^2}{r^2-1} F_3 - F_4} \{2r^2(F_1F_2-1) + \frac{r^4}{r^2-1} F_3F_6 - (1-r^2) F_4F_5\}$$

$$T_C = \frac{-iF_3F_4}{k(1-r^2)(\frac{r^2}{r^2-1} F_3-F_4)}$$

$$T_D = T_A \qquad (4.21)$$

4.2 Computation Results on Transmission Loss Curves

Expressions (4.13) are first tested on a plug muffler for which Sullivan [3] has presented experimental data on the perforate impedance and a transmission loss curve. The specific normal impedance of a perforated sample made of 0.81 mm thick plate with 4.2% open area has been measured by Sullivan to be,

$$\zeta = [6\times10^{-3} + i\ 4.8\times10^{-5}\ f]/\sigma \qquad (4.22)$$

in the linear range of particle-velocity through orifices, where f is the frequency in Hz and σ the fraction of open area. The test muffler for which Sullivan has presented a transmission loss curve, consists of a tube of diameter 49.3 mm, with centered plug and a uniform open area of 3.9%, enclosed in a chamber of diameter 101.6 mm and total length 257.2 mm. Figure 2 represents the theoretical and experimental

transmission loss curves for this plug muffler (all Figures, with the exception of Figure 1, found on page 4, will be shown in the Appendix). The agreement between the two curves is very good except for some differences near the primary resonance peak. The primary resonance frequency predicted by the expressions is about 100 Hz higher than the value from experiment. It is seen from equation (4.22) that for a frequency of 1000 Hz, the resistive part of the impedance is an order of magnitude lower than the reactive part. Figure 3 compares the transmission loss curves for the same muffler with and without perforate resistance. When perforate resistance is included, the maxima and the minima of the resonance peaks are lowered and raised slightly, respectively, the peak locations are unaffected.

We now proceed to investigate the contribution of each crossflow element to the transmission loss curve for the muffler.

A. Base Case: $\sigma_e = \sigma_c$; $\ell_e = \ell_c$

Figure 2 shows the transmission loss curves for the crossflow expansion, crossflow contraction, and the combined muffler. Since the lengths and the porosities of the two crossflow elements are the same, their transmission loss curves coincide exactly with each other as discussed earlier. The peaks of the curves for the two elements are seen to be located at identical frequencies--2050 Hz and 2600 Hz, resulting in peaks for the combined muffler at the same frequencies. It might also be noted that the transmission losses are always positive.

At this point, it is instructive to study the changes in contribution of the two crossflow elements to the overall transmission loss

curve, when the fractions of open area or the lengths are different for the two elements.

B. $\sigma_e \neq \sigma_c$; $\ell_e = \ell_c$

Figure 3 shows the curves for the muffler of Sullivan's work with one change: the fraction of open area on the tube after the plug is changed to .045. The curve for the crossflow expansion element shows peaks at 2050, and 2600 Hz just as before; the curve for the crossflow contraction element shows peaks at 2200 and 2700 Hz. That is, the difference in the peak locations for the two elements is maximum at the primary peak and diminishes progressively. The net result for the muffler transmission loss is that the effective width of the first peak is increased most, and the second less so. If the design objective were to broaden specific peaks, the difference in porosity would have to be picked carefully.

C. $\sigma_e = \sigma_c$; $\ell_e = \frac{3}{2} \ell_c$ (ℓ_e = 102.9 mm; ℓ_c = 154.3 mm)

Figure 5 shows the curves for this muffler with different lengths for the two elements. The curve for the crossflow expansion shows only 2 peaks--at 2050, 3050 Hz; the curve for the crossflow contraction shows 3 peaks--at 2150, 2350, and 3250 Hz. The net result is that the muffler transmission loss curve has resonance peaks at 4 locations; but the most noticeable difference between Figure 2 and Figure 5 is in the region of 2300 to 3500 Hz rather than near the primary resonance peak. It might be pointed out here that the combined muffler transmission loss is unaffected if the parameters for the crossflow expansion and the crossflow contraction are switched around.

Next, the effect of the porosity variation is studied on transmission loss curves for some test mufflers used at Nelson Industries. Since the perforate resistance with no mean for these mufflers is small and has not been available, only purely reactive impedance is used. The attached mass factors for these calculations was obtained from the unpartitioned concentric resonator studies reported by Jayaraman [2]. The agreement between theoretical result and the experimental result conducted at Nelson Industries is excellent for these plug mufflers at least in the prediction of resonance frequencies.

Figures 6 through 8 show the effect of porosity variation for Nelson mufflers with 1/8" holes on a 2" tube. When the porosity is changed from 4.81% to 2.405% uniformly along the tube, the transmission loss displays a trend similar to that observed for unpartitioned resonators--the resonance frequencies shift to lower values for the muffler with less open area. Figure 8 seems to indicate that if the two crossflow elements are of equal length but different porosities, the peaks on the transmission loss curves for the two elements while not coinciding, are close enough to result in broad peaks on the overall transmission loss curve. The spacing between peaks on the curves for the crossflow expansion and the crossflow contraction is maximum for the first peak and diminishes progressively for higher frequency peaks.

CHAPTER V

MODEL SIMULATIONS OF VARIOUS MUFFLER CONFIGURATIONS WITH MEAN FLOW

Transmission matrix expressions obtained in Chapter III are used to study the effect of parameters on TL curves for various muffler configurations with mean flow. As pointed out earlier, the decoupling approach requires a uniform mean flow inside the entire muffler; therefore, before the model is to be used, the incoming mean flow should be corrected to a lower average value for the muffler. The muffler configurations studied here include single plug mufflers, diffusers, and mufflers with more than one plug. The effect of various parameters, expecially porosity and chamber length, on TL curves is investigated for each configuration.

It has been well-known that the presence of mean flow tends to increase and decrease the resistance and reactance of the perforation, respectively. The simulations in this chapter are based on a uniform perforate impedance $\rho_0 c\zeta$ reported by Sullivan [3] from measurements on a sample with 4 percent open area, in the presence of mean flow. This impedance is given by

$$\zeta = (.514 \frac{d_1 M}{\ell\sigma} + i\ 4.8 \times 10^{-5} f)/\sigma \qquad (5.1)$$

where d_1, M, ℓ, σ and f are the tube diameter, Mach number, length of crossflow element, porosity and frequency (Hz), respectively.

The effect of various parameters on transmission loss curves for a number of muffler configurations is summarized below.

5.1 Plug Mufflers

(1) Base Case

The base case chosen here has the same dimensions as the one used in Chapter IV, except this time a mean flow Mach number of 0.05 is included. The muffler consists of a center plug with a uniform open area of 3.9% along a 49.3 mm diameter tube; the chamber diameter is 101.6 mm and the total length is 257.2 mm. Good agreement between the theoretical and the experimental results is observed for this muffler at 74°C (see Figure 9). This suggests that, in low Mach number, no correction is needed for the incoming mean flow to obtain good prediction. Figure 10 shows the TL curves for the same muffler at 22°C. We note that the TL curves for the crossflow expansion and the crossflow contraction chambers coincide with each other; also, as temperature decreases, the resonance peaks shift to lower frequencies. 22°C is used for all the following computer simulations.

(2) Effect of Porosity Change $\ell_e = \ell_c$

Figure 11 shows the TL curves for the same muffler but with one change: the fraction of open area for the crossflow contraction element is increased to 4.5%. As a result, the sound attenuation for this element decreases slightly due to this change, the overall sound attenuation for the muffler is also decreased.

Figures 12 to 15 present some interesting results from our analysis, on the interaction between effects of porosity and of mean flow.

These

and t

2, 3

for

on t

2% p

incr

freq

of

pea

inv

inc

How

att

se

co

ef

ne

on

lo

nu

fo

These curves are calculated using the same impedance model (as in (5.1)) and the same lengths and diameters for M=0 and M=.05 with porosities of 2, 3, 4 and 5 percent. The maximum effect of the mean flow is observed for the plug muffler with the lowest porosity in that the peak magnitudes on the transmission loss curves for M=0 and .05 are farthest apart with 2% porosity; this difference decreases consistently as the porosity is increased. Moreover, while for M=0, the resonance peaks shift to higher frequencies with increasing porosity as expected, for M=.05, the locations of the peaks are insensitive to porosity. Only the magnitudes of the peaks diminish significantly with increasing porosity for M=.05.

From equation (5.1), the resistance component of impedance is inversely proportional to porosity; the above analysis shows that an increase in resistance causes the sound attenuation to be increased. However, in the cases for M=0, as described in Chapter III, the sound attenuation decreases slightly when resistance is included.

(3) Effect of Plug Location

Figure 16 shows the TL curves for the base case muffler with offset plug; the lengths for the crossflow expansion and the crossflow contraction are 85.7 mm and 171.5 mm, respectively. In contrast to the effect of porosity variation, varying the lengths of the crossflow elements affects mostly the peak locations and the sound attenuations are only slightly affected. Since the crossflow contraction element is longer than the crossflow expansion element, it shows more peaks. The number of peaks for the overall TL curve is roughly the sum of the peaks for the two crossflow elements. However, the peaks of the crossflow

elements do

sharply as

(4) Ser

Figu

(a) the ex

mean flow

mean flow

at room te

.15. It

sions pro

curves di

reported

computed

are very

curve ob

tube and

term.

5.2 Diff

A

ing of a

inlet ar

chamber

entrance

cross-se

the emp

elements do not coincide with the peaks of the overall TL curves as sharply as in the cases when M=0.

(4) Sensitivity of TL Curves to Convective Term

Figure 17 presents the transmission loss curves computed using (a) the expressions in (3.41) incorporating the convective effect of mean flow and (b) the expressions in (4.13) and (4.17) involving the mean flow only in the perforate resistance, for the base case muffler at room temperature over a range of Mach numbers - M = .01, .05 and .15. It may be noted that for M = .01 and .05, the two sets of expressions provide very nearly the same results while the M = .15, the two curves differ in peak magnitudes by up to 30 percent. Sullivan has reported (Figure 10 of [3], Part II) that the transmission loss curves computed with and without convective effects (using a segmental analysis) are very close even at M = .15. However, experimental transmission loss curve obtained at Nelson Industries for a plug muffler with a ¼" hole tube and 5% porosity agrees very well with our model with convective term.

5.2 Diffusers

A diffuser (see Figure 18) is a common silencing device consisting of a crossflow expansion chamber followed by an empty chamber. The inlet and the outlet diameters are assumed to be the same. The empty chamber can be modeled by a straight pipe with an abrupt expansion entrance and an abrupt contraction exit. However, in most cases, the cross-sectional areas of the annulus in the crossflow expansion and of the empty chamber do not differ greatly; therefore, the effect of the

abrupt expansion is small and can be neglected.

The transmission matrix for the empty chamber can be modeled as

$$\begin{pmatrix} P_{2a} \\ \rho c v_{2a} \end{pmatrix} = \underline{\underline{T}}_p \, \underline{\underline{T}}_c \begin{pmatrix} P_{1b} \\ \rho c v_{1b} \end{pmatrix} \tag{5.3}$$

where $\underline{\underline{T}}_p$ and $\underline{\underline{T}}_c$ are the transmission matrices for the straight pipe and the sudden contraction, respectively. The matrix parameters for the straight pipe are given by

$$\underline{\underline{T}}_p = \begin{bmatrix} T_{Ap} & T_{Bp} \\ T_{Cp} & T_{Dp} \end{bmatrix} \tag{5.4}$$

where

$$\begin{aligned} T_{Ap} &= F \cdot \cos \alpha \\ T_{Bp} &= i.F \cdot \sin \alpha \\ T_{Cp} &= T_{Bp} \\ T_{Dp} &= T_{Ap} \\ \alpha &= k\ell/(1-M^2) \\ F &= \cos(\alpha M) - i \sin(\alpha M) \end{aligned} \tag{5.5}$$

The matrix parameters of the sudden contraction (see [4]) are given by

$$\underline{T}_C = \begin{bmatrix} T_{Ac} & T_{Bc} \\ T_{Cc} & T_{Dc} \end{bmatrix} \tag{5.6}$$

where

$$T_{Ac} = G\cdot\left(\frac{1}{A_1} - \frac{M^2 A_2}{A_1^2}\right)$$

$$T_{Bc} = G.M.\left(\frac{1}{A_1 A_2^2} - \frac{1}{A_1^2 A_2}\right)$$

$$T_{Cc} = G\cdot M\cdot(A_2 - A_1)$$

$$T_{Dc} = G\cdot\left(\frac{1}{A_2} - \frac{A_1\cdot M^2}{A_2^2}\right)$$

$$G = \frac{A_1}{1-M^2} \tag{5.7}$$

A_1 and A_2 are the cross-sectional areas of the tube and the chamber, respectively.

The transmission loss curves for three diffusers with different plug locations are plotted in Figures 19 to 21. It is apparent from these figures that the higher peaks in the overall TL curves correspond to peaks of TL in the crossflow element, while peaks of TL in the empty chamber contribute to the shorter peaks in the overall TL curves. As the plug is shifted closer to the outlet of the diffuser, the peaks of TL in the longer crossflow element are shifted to lower frequencies while the peaks of TL in the shorter empty chamber section are shifted to higher frequencies so that in net effect, the higher peaks of overall TL are obtained at lower frequencies and the shorter peaks at higher frequencies. Next, comparing Figure 10 for a center plug muffler with two crossflow elements and Figure 19 for a center plug diffuser, it may

be seen that while plateaus or incomplete humps occur on the TL curve for the plug muffler between crossflow resonance frequencies; for the diffuser, complete loops with sharp minima are obtained on the TL curve between crossflow resonance frequencies. The effect of porosity in the presence of mean flow is the same as discussed for plug mufflers: decrease in porosity increases the magnitude of sound attenuation, but the peak locations remain unchanged.

5.3 Two-plug Mufflers

We now study the utility of inserting more than one plug in the center tube. Again, a mean flow Mach number of 0.05 is assumed for all cases to be studied here. Two configurations are considered: one consisting of four consecutive crossflow elements, and the other consisting of two crossflow elements separated by an empty region.

(1) Two-plug Mufflers in Series

Another common exhaust system design is the series connection of two or more plug sections (see Figure 22). We study here the simplest case in which only two plug sections are connected resulting in a total of four crossflow elements (see Figure 23). The transmission matrix expressions for this muffler can be obtained simply from multiplying the transmission matrices of two simple plug mufflers together. An advantage of this design is to provide more freedom in selecting the crossflow element lengths.

We first put two of our base case mufflers together. The combined muffler consists of two identical plug sections, each plug section has a center plug and a total length of 257.2 mm. In Figure 24, curve A

represents the TL curve for the combined muffler, and curve B represents the TL curve for either the first or the second plug sections since the two-plug sections are of identical configuration. As might be expected, most of the peaks for curve A have magnitudes of sound attenuation of approximately twice and located just on the top of the peaks of curve B. The combined muffler provides higher sound attenuation than a single plug section; however, it is also longer and costs more to be manufactured.

We proceed to a more meaningful comparison of 2-plug and 1-plug mufflers, keeping the same total length. Figure 25 shows the TL curves for a combined muffler similar to the one described above except with one change: each crossflow element is reduced to 64.3 mm long. As before, the upper curve C represents the TL curve for the combined muffler, the lower curve D represents the TL curves for either the first or the second plug sections. It is informative to compare curve B in Figure 24 with curve C in Figure 25 since the mufflers representing these curves have the same total length of 257.5 mm. The difference between these two curves: curve B represents a single plug muffler with two crossflow elements; curve C represents a combined muffler with four crossflow elements, each crossflow element is half as long as the ones in curve B. Comparing to curve B, since curve C has shorter crossflow elements, it has fewer peaks and its primary peak occurs at a higher frequency; on the other hand, since it has more crossflow elements of equal length, the TL peaks of its crossflow elements coincide to provide higher sound attenuation.

We proceed further to study the behavior of our combined muffler with different plug section lengths. Figure 26 represents the TL curves for a combined muffler which has two center plug sections with unequal lengths, the lengths for the first and the second plug sections are 128.6 mm and 257.2 mm, respectively. As a result, the TL curves for the peaks of the two-plug sections do not coincide with each other, but some of them are close enough to create broad peaks on the overall transmission loss curve.

So far, the plug sections studied all have center plugs. When offset plug sections are selected carefully, a broader band of attenuation can be obtained. For example, Figure 27 shows the TL curves for a muffler with progressively increasing lengths for its four crossflow elements. The lengths of the crossflow elements are 40 mm, 56 mm, 72 mm, and 88 mm. As a result, the peaks of the crossflow elements are so close to one another that a very broad band of attenuation can be observed in the overall TL curve.

(2) Empty Region Between Two Crossflow Elements

We now study another 2-plug muffler where an empty region is inserted between the crossflow expansion and the crossflow contraction elements (see Figure 28). The effect of the sudden expansion and the sudden contraction before and after the empty region is small and is neglected here. Hence, the transmission matrix for this empty region can be represented by equation (5.5).

We proceed to study the effect of varying the length of this empty region on TL curve. Figure 29 represents the TL curves for this kind of

muffler with a gap of 21.43 mm, the ratio between the lengths of the crossflow expansion, the empty region, and the crossflow contraction is 5.5:1.0:5.5. The transmission loss for the empty region is nearly zero for the entire frequency range. Comparing to the overall TL curve of the base case (see Figure 10) which has no gap, the peaks of the overall TL in Figure 29 occur at higher frequencies.

To see the effect of the empty region more clearly, we take the muffler in Figure 29, deleting its empty region, and study the overall TL curves of the two crossflow elements. The TL curves of this muffler, which has a shorter total chamber length of 235.76 mm, is shown in Figure 30. For small gaps, it appears that the empty region has only a slight effect on the overall TL curve.

However, a larger gap can change the overall TL curve more. Figures 31 and 32 show the TL curves for two mufflers with gap lengths of 42.87 mm and 64.29 mm respectively. As the gap becomes longer, the lengths of the crossflow elements become shorter, and the resonance peaks are shifted to higher frequencies. It is observed that there is a broad band of sound attenuation in the frequency range from 2100 Hz to 3400 Hz. The peak magnitudes and the total number of peaks for the overall TL curve remain unchanged when the length of the gap is varied.

CHAPTER VI

PREDICTION OF RESONANCE FREQUENCIES IN THE ABSENCE OF MEAN FLOW

A strikingly simple and useful description of perforated tube components may be obtained from the expressions in Chapter IV for the case with no mean flow using a purely reactive perforate impedance: $\zeta = i\chi/\sigma$. For a reactive perforate we may write

$$\chi = k\Delta \text{ so that } \zeta = ik\Delta/\sigma \tag{6.1}$$

where Δ is the effective length of oscillating gas column in the perforations, determined from the thickness of the tube wall, t and the hole diameter d_o with attached mass factor A by $\Delta = t + A\, d_o$. Combining (6.1) and (3.22) shows that

$$(k_1\ell)^2 = (k\ell)^2 - (\psi\ell)^2 \; ; \; \left[(\psi\ell)^2 \equiv \frac{4\sigma}{d_1\Delta}\ \frac{\ell^2}{1-r^2}\right] \tag{6.2}$$

The parameter $(\psi\ell)^2$ is a dimensionless group incorporating all the geometric parameters of a resonator with real values and hence $(k_1\ell)^2$ is real; $k_1\ell$ itself will be real only if

$$(k\ell)^2 > (\psi\ell)^2 \tag{6.3}$$

Looking back at equations (4.4) and (4.5) (with M=0) in the light of condition (6.3) leads to clear insight into high frequency resonances of perforated elements. If $k_1\ell$ is imaginary (i.e., $(k\ell)^2 < (\psi\ell)^2$), and

of order 1, Γ_1 is attenuated while Γ_2 propagates with wavenumber k. However, if $k_1\ell$ is real, Γ_1 will be propagated without attenuation, recalling here that Γ_1 is directly related to the radial velocity fluctuation shows that the transmission loss at higher frequencies corresponding to $k^2 > \psi^2$ must be influenced by the propagation of radial velocity fluctuations through the holes. As an illustration, consider an unpartitioned resonator 1 ft long consisting of a 2.125 in tube with 1/4 in holes amounting to 4.9 percent porosity, in a 5.56 in chamber with Δ = .245 in; for this resonator, condition (6.3) yields the frequency range f > 1440 Hz in which the propagation of radial velocity fluctuations determines the resonance peaks.

We proceed to show that the resonance frequencies for a reactive plug muffler may be obtained accurately with a simple formula involving the dimensionless group $(\psi\ell)^2$. Let us begin by noting that the resonance frequencies for a plug muffler after the expansion chamber humps coincide with the peak frequencies of the crossflow elements comprising the plug muffler. This may be seen in Figure 4 for a muffler with different porosities before and after the plug; and in Figure 33 for another muffler with different lengths before and after the plug. Hence it suffices to look at the transmission loss peaks of crossflow elements. Extensive simulation of reactive crossflow elements reveals that the resonance frequencies of a crossflow element may be obtained by setting the common denominator of the expressions in (4.13) to zero. This yields

$$k_{o,n}\ell \sin k_{o,n}\ell - \sqrt{k_{o,n}^2\ell^2-\psi^2\ell^2} \sin \sqrt{k_{o,n}^2\ell^2-\psi^2\ell^2} = 0 \quad (6.4)$$

with

$$k_{o,n} \equiv \frac{2\pi}{c} \left[\begin{matrix}\text{nth resonance frequency} \\ \text{for crossflow element}\end{matrix}\right].$$

The solutions to equations (6.4) have been plotted in Figure 34 as straight lines (one for each n) relating $k_{o,n}\ell$ to $\psi^2\ell^2$ according to

$$k_{o,n}\ell = a_n (\psi\ell)^2 + b_n \tag{6.5}$$

where the coefficients for the first four resonance peaks are

$$\begin{aligned} a_1 &= 0.1046 & b_1 &= 2.1011 \\ a_2 &= 0.0430 & b_2 &= 4.9913 \\ a_3 &= 0.0298 & b_3 &= 8.0012 \\ a_4 &= 0.0219 & b_4 &= 11.1035 \end{aligned} \tag{6.6}$$

over the range of $(\psi\ell)^2$ between 0 to 40. This range includes a substantial variety of geometric parameters. To illustrate, let us take the crossflow contraction from the example of Figure 4 for which $(\psi\ell)^2 = 30$ and the resonance frequencies may be determined accurately (to within 5 Hz) from Figure 34 as 2234 Hz, 2678 Hz, and 3792 Hz. These frequencies may be verified on the transmission loss curve for the crossflow contraction in Figure 4 obtained by using the complete model expressions. In another example of the crossflow expansion treated in Figure 33, $(\psi\ell)^2 = 11.48$ and the resonance frequencies are once again predicted accurately from Figure 34 as 1430 Hz, 2374 Hz and 3612 Hz. These frequencies may be verified on the transmission loss curve for the crossflow expansion in Figure 33.

Equation (6.5) allows us to see clearly the effect of various geometric parameters on the resonance frequencies.

Recalling $(\psi\ell)^2 = \frac{4\sigma}{d_1\Delta} \frac{\ell^2}{1-r^2}$, as the diameter of the center tube is increased, the peaks will shift to lower frequencies as long as $\frac{1}{1-r^2}$ does not increase much. As the diameter of the chamber is increased, the peaks will also shift to lower frequencies. As the porosity is increased, the peaks will shift to higher frequencies. As the hole diameter is increased, Δ will increase leading to lowering of the peak frequency locations.

The effect of varying the length of the crossflow element is a little more involved. From equation (6.5), the resonance frequencies can be obtained as

$$f_{o,n} = \frac{c}{2\pi} \left[a_n \psi^2 \ell + \frac{b_n}{\ell}\right] \tag{6.7}$$

where $f_{o,n}$ is a convex function of the chamber length ℓ because $a_n>0$, $b_n>0$, for all n. The minimum of this convex function can be identified easily for each resonance peak as

$$\ell_{min,n} = \frac{b_n}{a_n} \frac{1}{\psi} \tag{6.8}$$

For $\ell < \ell_{min,n}$, an increase in length will shift the resonance peaks to lower frequencies; for $\ell > \ell_{min,n}$, an increase in length will shift the resonance peaks to higher frequencies; also, the lowest resonance frequency for a given ψ occurs at $\ell_{min,n}$. As an example, we use some Nelson Industries experimental TL curves (Figures 34 to 38) for plug mufflers to illustrate this point. Table 1 presents the first resonance peaks for these plug mufflers with different offsets. $(\psi\ell)^2$ varies from 3.9 to 35.5. The agreement between the resonance peaks predicted from

TABLE I

Primary resonance frequencies obtained from experiment and the simple relation for mufflers in Figures 35 through 38

Length of Cross-flow Element	$(\psi\ell)^2$	Primary Resonance Frequencies	
		Experiment	Simple Relation
3 in.	3.9	1800	1814
4 in.	7.0	1550	1534
5 in	11.0	1450	1406
6 in.	15.8	1350	1354
7 in.	21.5	1350	1345
8 in.	28.1	1360	1363
9 in.	35.5	1430	1399

our simple relation and the experimental result is excellent. $\ell_{min,1}$ is calculated from equation (6.8) to be 6.77 in, and the lowest experimental frequency resonance peaks also occurs at this length.

The trends described above are most noticeable in the first resonance peak. It may be noted from equation (6.8) that with increasing n, the effect of geometric parameters, except for the length, is diminished.

The question arises at this point of how the model simplification might be extended to mufflers with large perforate resistance, in the presence of mean flow. For such cases, $(k_1\ell)^2$ is complex and attempts at deriving simple predictors of resonance frequencies have so far been unsuccessful. It remains for future work to find an appropriate analogue to equation (6.3) which would provide good estimates of resonance frequencies for crossflow resonators with mean flow.

CHAPTER VII

CONCLUSIONS

A new approach has been described for solving problems of plane wave propagation in multiduct configurations with the same mean flow in the ducts by decoupling the differential equations. This approach leads to compact expressions for matrix parameters and transmission loss without any concern for convergence of infinite series or segmental analysis employed in earlier studies. The predicted transmission loss curves agree very well with published data of Sullivan [3] for plug mufflers with M = 0 and M = .05.

The predicted transmission loss curves for plug mufflers in the absence of mean flow agree very well with the experimental results obtained at Nelson Industries. The resonance frequencies for a plug muffler after the expansion chamber humps coincide sharply with the peak frequencies of the crossflow elements comprising the plug muffler. By varying the plug location and porosity, resonance peaks of different frequencies and width can be obtained.

Although the decoupling analysis requires the mean flows in the two ducts be the same, this assumption does not appear to be a restriction in predicting observed behavior if an average value, less than the incoming mean flow, is chosen for the mean flow in the two ducts. Moreover, for Mach numbers at least up to 0.16 the perforate resistance

may be adjusted to obtain a good prediction, without convective terms in the model.

The following trends of geometric variation on TL curves for crossflow elements with mean flow are observed. On one hand, as length is increased, the resonance peaks are shifted to lower frequencies resulting in more peaks within a given frequency range; however, the magnitude of sound attenuation is relatively insensitive to length variation. On the other hand, variation of porosity creates an opposite effect: as porosity is decreased, there is almost no effect on the peak locations, but the sound attenuation is increased. Providing that the pressure loss is within available limits, low porosity is recommended for obtaining high sound attenuation.

In our study of the performance of various configurations--plug mufflers, diffusers and plug mufflers with gaps, the approach of comparing the overall transmission loss curves with the TL curves for each of the elements comprising these mufflers has consistently yielded useful insight by allowing us to identify the contributions of various elements to the overall performance.

Within the same total length and muffler volume as a single plug muffler, the combination of two-plug mufflers involving four crossflow elements can achieve either a broader band of sound attenuation or higher peaks. A broader band of sound attenuation can be achieved by choosing different crossflow element lengths, and higher peaks can be achieved by choosing the crossflow elements to have the same length. This type of muffler provides a more selective and economical design. However, the major drawback is its excessive aerodynamic blockage

created by more plugs which might make this design impractical in some cases.

The decoupled equations also clarify the connection between high frequency resonances of perforated elements and the axial propagation of radial velocity fluctuations through the holes, without mean flow. In addition, the resonance frequencies of a plug muffler are seen to coincide with the resonance frequencies of crossflow elements which in turn may be correlated very simply and accurately with the dimensionless group $(\psi\ell)^2$ defined in this work. This correlation bears out all the trends observed with variation of geometric parameters. Although these correlations are obtained by assuming purely reactive mufflers, perforate resistance without mean flow is too small to affect the peak locations. Analogous, simple correlations of resonance frequencies for the largely resistive crossflow elements with mean flow, are not yet available.

For future work, the decoupling approach may be extended to describe mufflers with more than two ducts. Experimental data on impedance measurements is also needed for more extensive simulations.

REFERENCES

REFERENCES

1. J. W. Sullivan and M. J. Crocker, J. Acoust. Soc. Am. 64, (1), 207 (1978).

2. K. Jayaraman, "Modeling Study of Concentric Resonators Performance Using Transfer Function Measurement," Research Report to Nelson Industries, Inc., September, 1979.

3. J. W. Sullivan, J. Acoust. Soc. Am. 66, (3), 772 (Part I & II) (1979).

4. J. W. Sullivan, "Modeling of Engine Exhaust System Noise," in Noise and Fluids Engineering. Proceedings of Winter Annual Meeting of the American Society of Mechanical Engineers, edited by Hickling (Atlanta, 1977), pp. 161-169.

5. T. H. Melling, Journal of Sound and Vibration 29, 1, p. 1 (1973).

APPENDIX

APPENDIX

$\{\tau_j\}$ EXPRESSIONS FOR EQUATIONS (3.38) and (3.40)

The following relations hold for the $\{\tau_j\}$ appearing in equations (3.38) and (3.40).

$$\tau_1 = \{A_2[1 - \frac{\phi_1}{E} e^{-i\phi_1 \ell} (\frac{1}{\phi_3} + \frac{1}{\phi_4})] - A_1 \frac{\phi_1}{E} [\frac{e^{i\phi_4 \ell}}{\phi_3} + \frac{e^{-i\phi_3 \ell}}{\phi_4}]\} / A_K \tag{A1}$$

$$\tau_2 = \{A_2[1 + \frac{\phi_2}{E} e^{i\phi_2 \ell} (\frac{1}{\phi_3} + \frac{1}{\phi_4})] + A_1 \frac{\phi_2}{E} [\frac{e^{i\phi_4 \ell}}{\phi_3} + \frac{e^{-i\phi_3 \ell}}{\phi_4}]\} / A_K \tag{A2}$$

$$\tau_3 = \{A_2 \phi_1[\frac{1}{k-M\phi_1} - \frac{e^{-i\phi_1 \ell}}{E} (\frac{1}{k-M\phi_3} - \frac{1}{k+M\phi_4})] - A_1 \frac{\phi_1}{E} [\frac{e^{i\phi_4 \ell}}{k-M\phi_3} - \frac{e^{-i\phi_3 \ell}}{k+M\phi_4}]\} / A_K \tag{A3}$$

$$\tau_4 = \{-A_2 \phi_2[\frac{1}{k+M\phi_2} - \frac{e^{i\phi_2 \ell}}{E} (\frac{1}{k-M\phi_3} - \frac{1}{k+M\phi_4})] + A_1 \frac{\phi_2}{E}[\frac{e^{i\phi_4 \ell}}{k-M\phi_3} - \frac{e^{-i\phi_3 \ell}}{k+M\phi_4}]\} / A_K \tag{A4}$$

$$\tau_5 = \{-A_2 \frac{\phi_1}{E} e^{-i\phi_1 \ell}[\frac{e^{-i\phi_3 \ell}}{\phi_3} + \frac{e^{i\phi_4 \ell}}{\phi_4}] - A_1[e^{-i\phi_1 \ell} + \frac{\phi_1}{E} e^{i(-\phi_3+\phi_4)\ell}(\frac{1}{\phi_3} + \frac{1}{\phi_4})]\} / A_K \tag{A5}$$

$$\tau_6 = \{A_2 \frac{\phi_2}{E} e^{i\phi_2 \ell}[\frac{e^{-i\phi_3 \ell}}{\phi_3} + \frac{e^{i\phi_4 \ell}}{\phi_4}] - A_1[e^{i\phi_2 \ell} - \frac{\phi_2}{E} e^{i(-\phi_3+\phi_4)\ell}(\frac{1}{\phi_3} + \frac{1}{\phi_4})]\}/A_K \quad \text{(A6)}$$

$$\tau_7 = \{-A_2[\frac{\phi_1}{E} e^{-i\phi_1 \ell}(\frac{e^{-i\phi_3 \ell}}{k-M\phi_3} - \frac{e^{i\phi_4 \ell}}{k+M\phi_4})] - A_1 \phi_1[\frac{e^{-i\phi_1 \ell}}{k-M\phi_1} + \frac{e^{i(-\phi_3+\phi_4)\ell}}{E}(\frac{1}{k-M\phi_3} - \frac{1}{k+M\phi_4})]\}/A_K \quad \text{(A7)}$$

$$\tau_8 = \{A_2 \frac{\phi_2}{E} e^{i\phi_2 \ell}[\frac{e^{-i\phi_3 \ell}}{k-M\phi_3} - \frac{e^{i\phi_4 \ell}}{k+M\phi_4}] + A_1 \phi_2[\frac{e^{i\phi_2 \ell}}{k+M\phi_2} + \frac{e^{i(-\phi_3+\phi_4)\ell}}{E}(\frac{1}{k-M\phi_3} - \frac{1}{k+M\phi_4})]\}/A_K \quad \text{(A8)}$$

$$A_K \equiv \pi(d_2^2 - d_1^2)/4$$

$$E \equiv e^{-i\phi_3 \ell} - e^{i\phi_4 \ell}$$

$$A_1 \equiv \begin{cases} \pi d_1^2/4 & \text{for expansion} \\ A_K & \text{for contraction} \end{cases} \quad \text{(A9)}$$

$$A_2 \equiv \begin{cases} A_K & \text{for expansion} \\ \pi d_1^2/4 & \text{for contraction} \end{cases}$$

FIGURE CAPTIONS

Unless specified otherwise, the following may be assumed:

- o overall muffler
- ▲ crossflow expansion
- ▼ crossflow contraction

d_1 = 49.3 mm; d_2 = 101.6 mm;

total length = 257.2 mm; $\sigma_e = \sigma_c$ = .039.

For diffusers (Figures 19 through 21)

- o overall
- ▲ crossflow expansion
- —— straight pipe

For two-plug muffler in series (Figures 24 through 27)

- o overall
- ▲ first plug section
- ▼ second plug section

3.9% uniform porosities

For mufflers with an empty space between two crossflow elements (Figures 29, 31, 32)

- o overall
- ▲ crossflow expansion
- ▼ crossflow contraction
- —— straight pipe

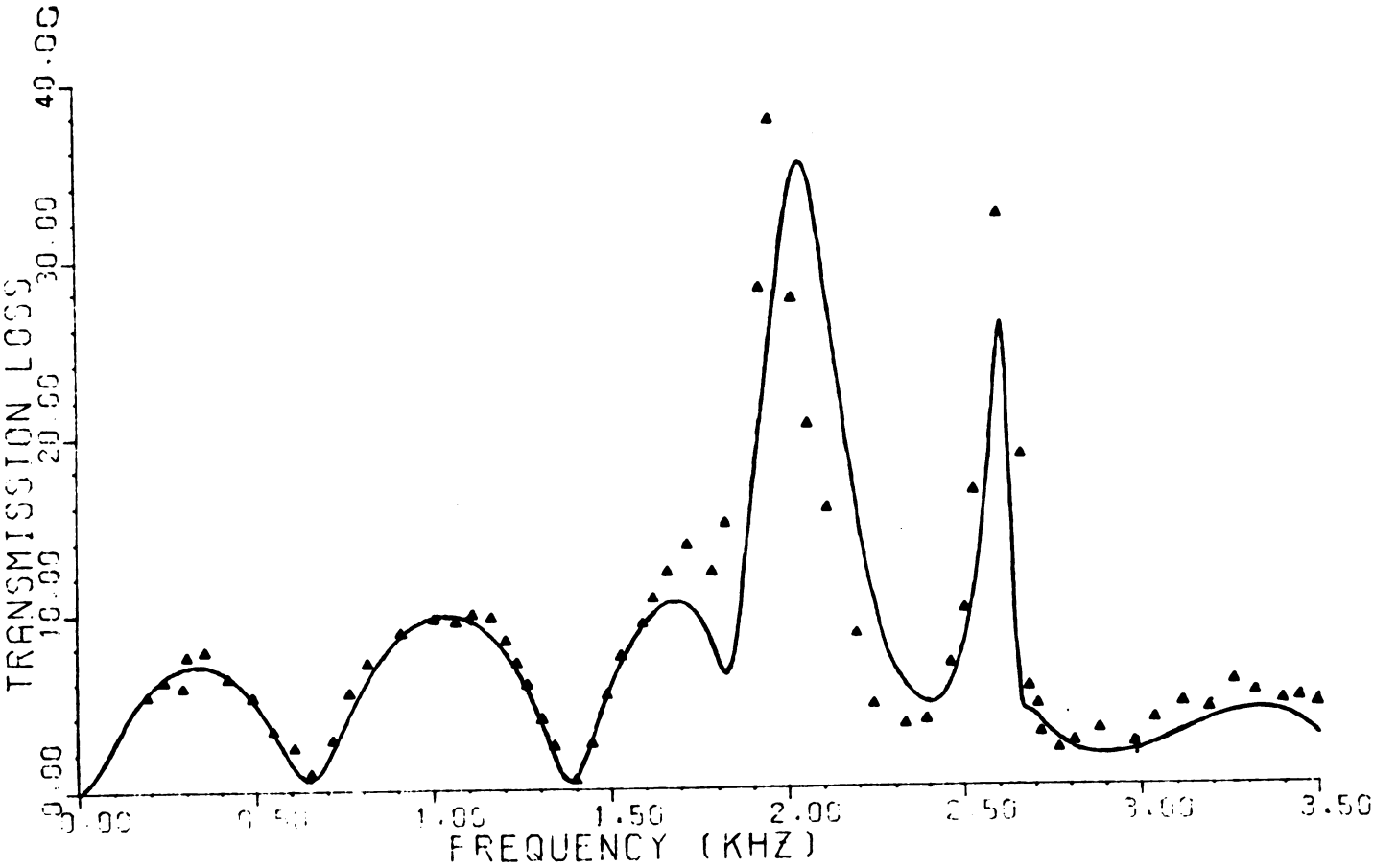

Figure 2. Plug muffler: center plug, $\sigma_c = \sigma_e = .039$, M = 0.
▲ experimental data points.

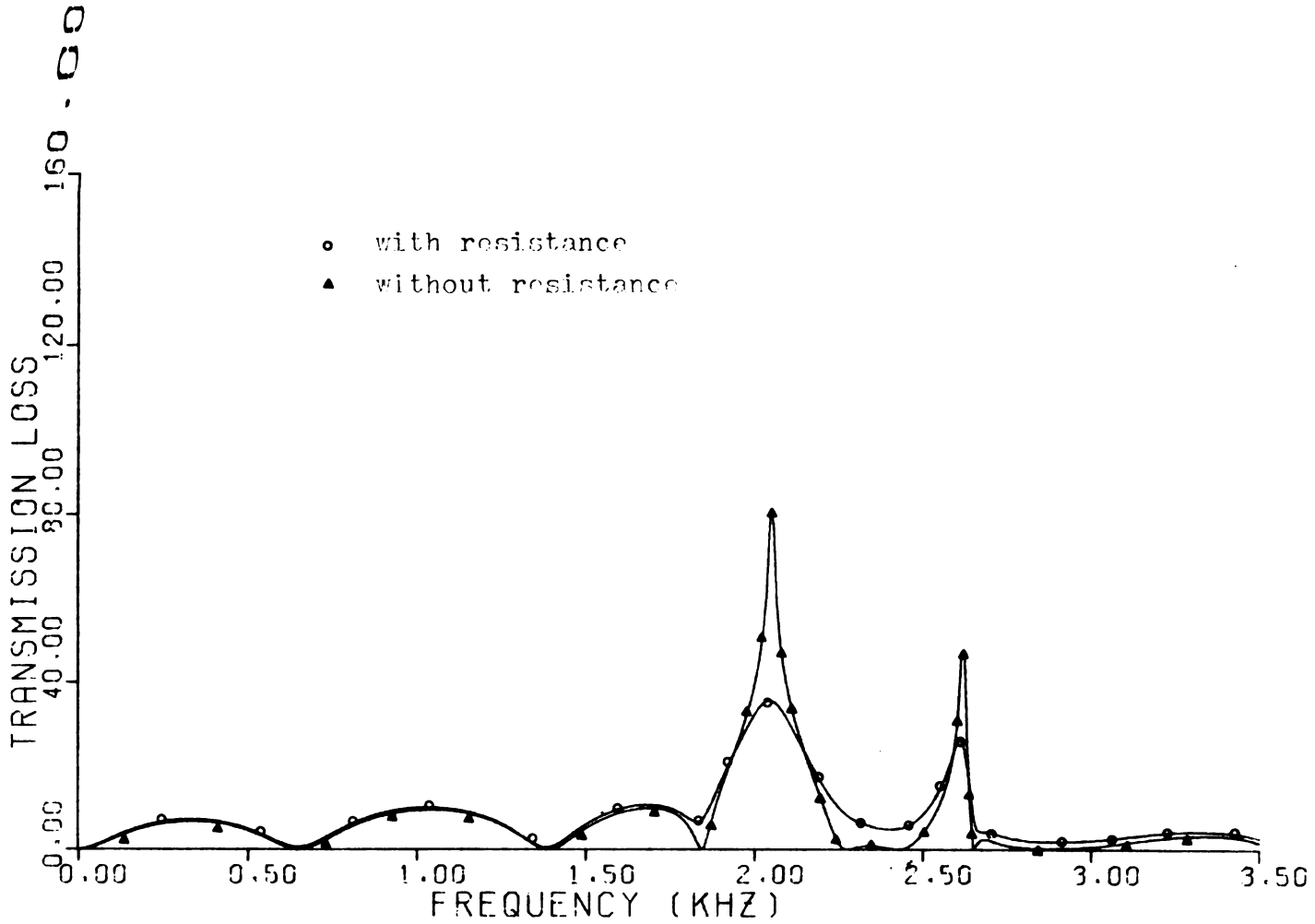

Figure 3. Comparison of TL curves for plug muffler with and without perforate resistance term. $\sigma_c = \sigma_e = .039$; M = 0.

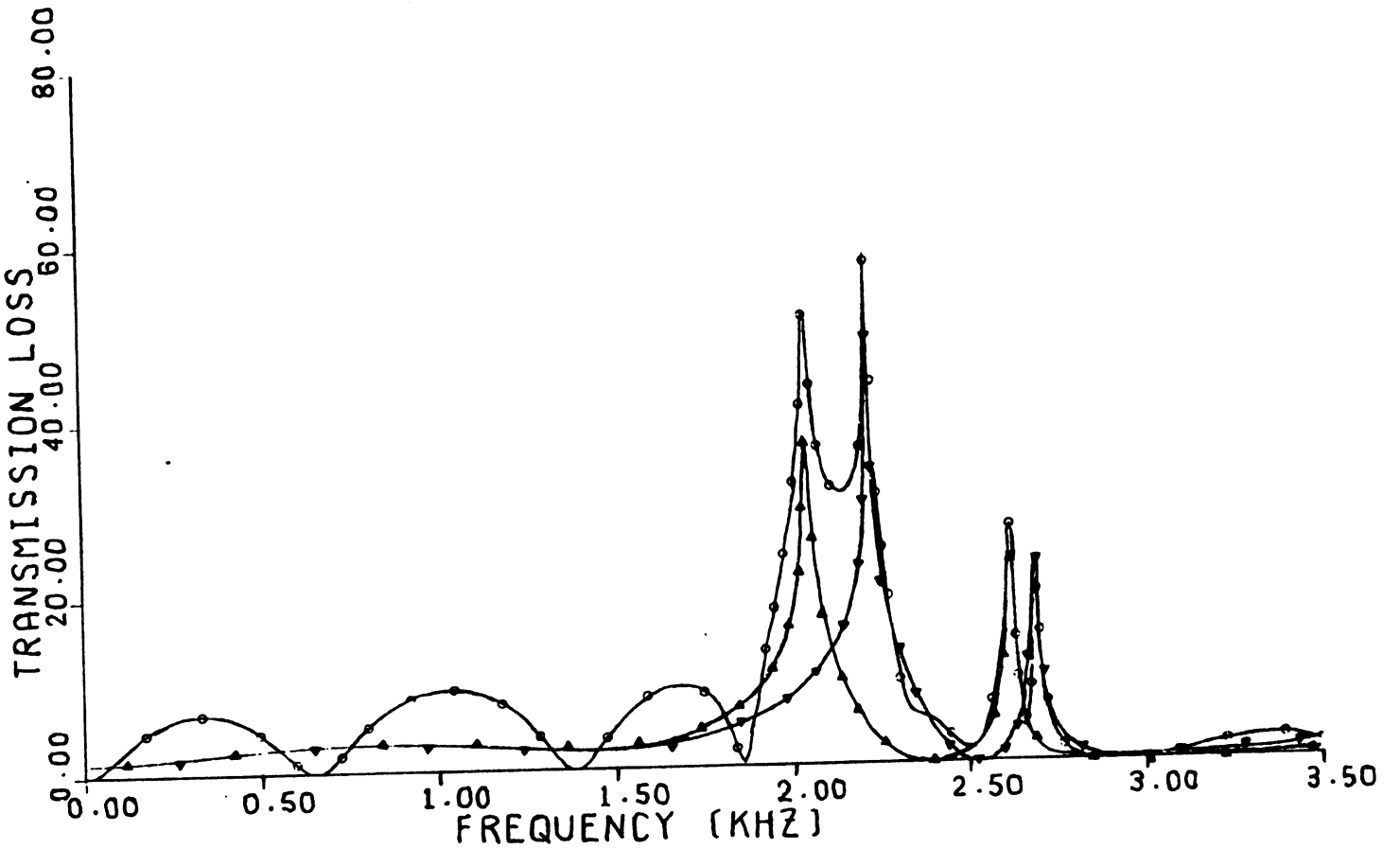

Figure 4. Plug muffler different porosities, σ_c = .039, σ_c = .045; M = 0.

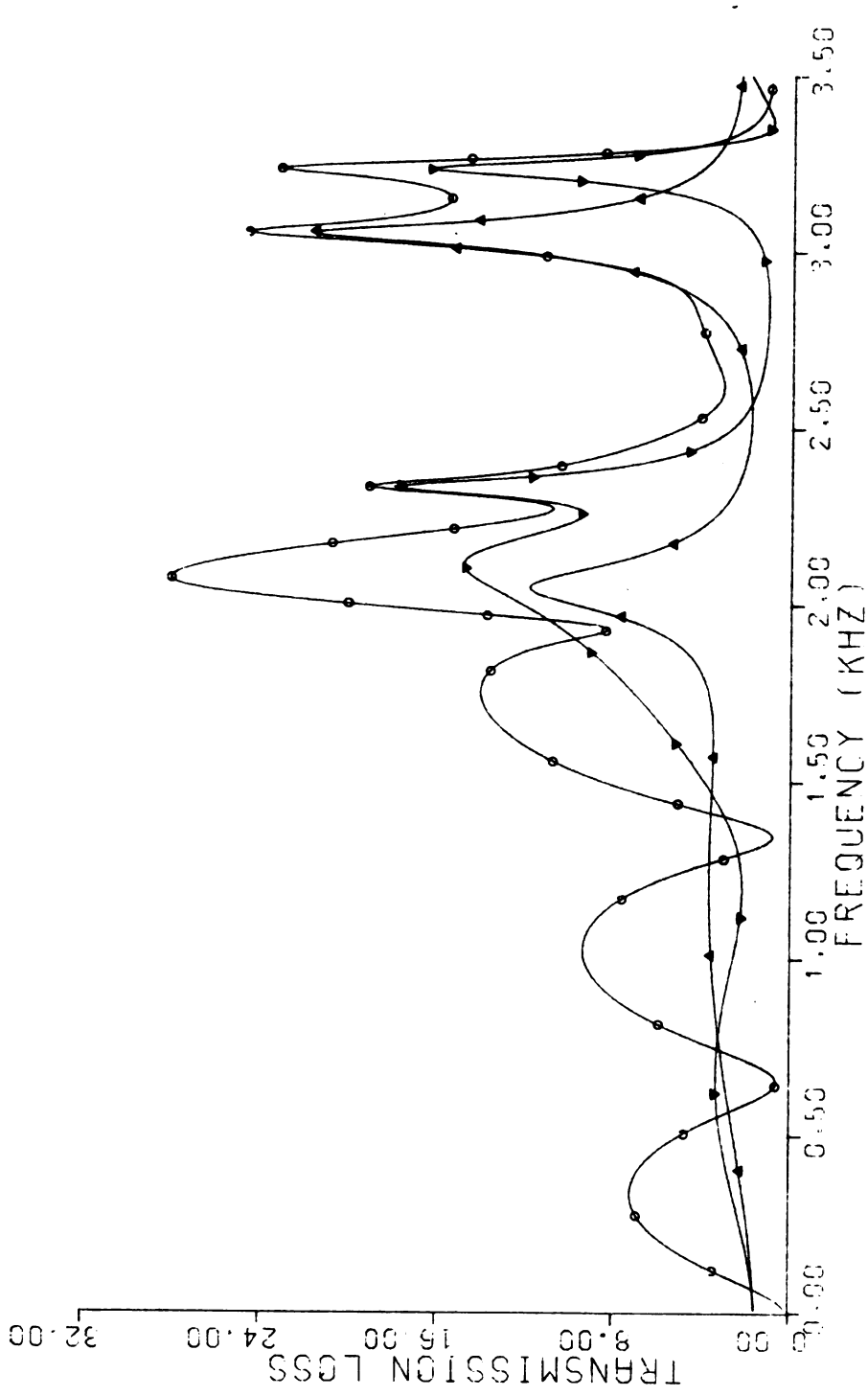

Figure 5. Plug muffler: offset plug, ℓ_e = 102.9 mm; ℓ_c = 154.3 mm; M = 0.

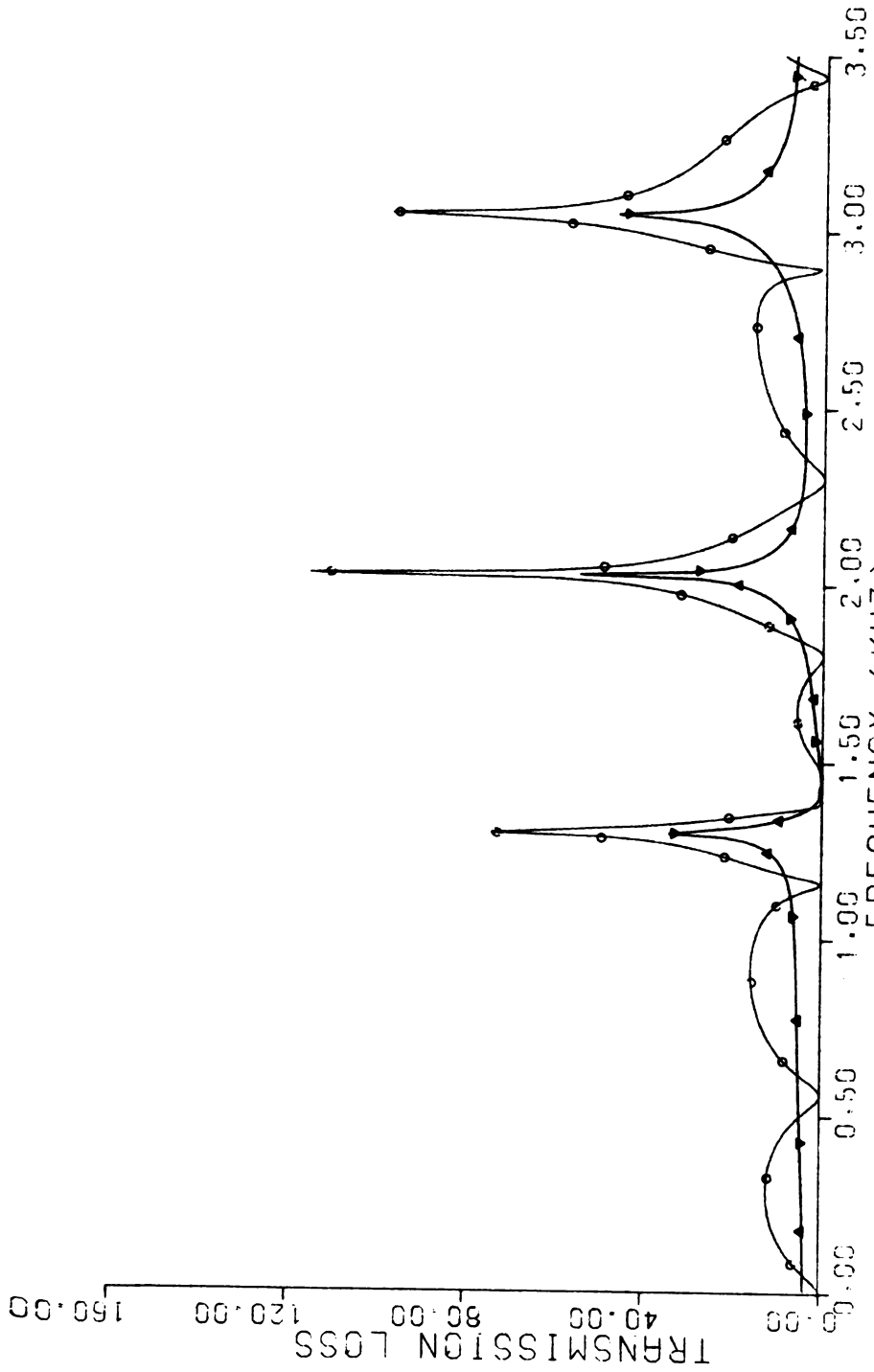

Figure 6. Plug muffler: $\ell_e = \ell_c = 6$ in, $\sigma_e = \sigma_c = .02405$; M = 0.

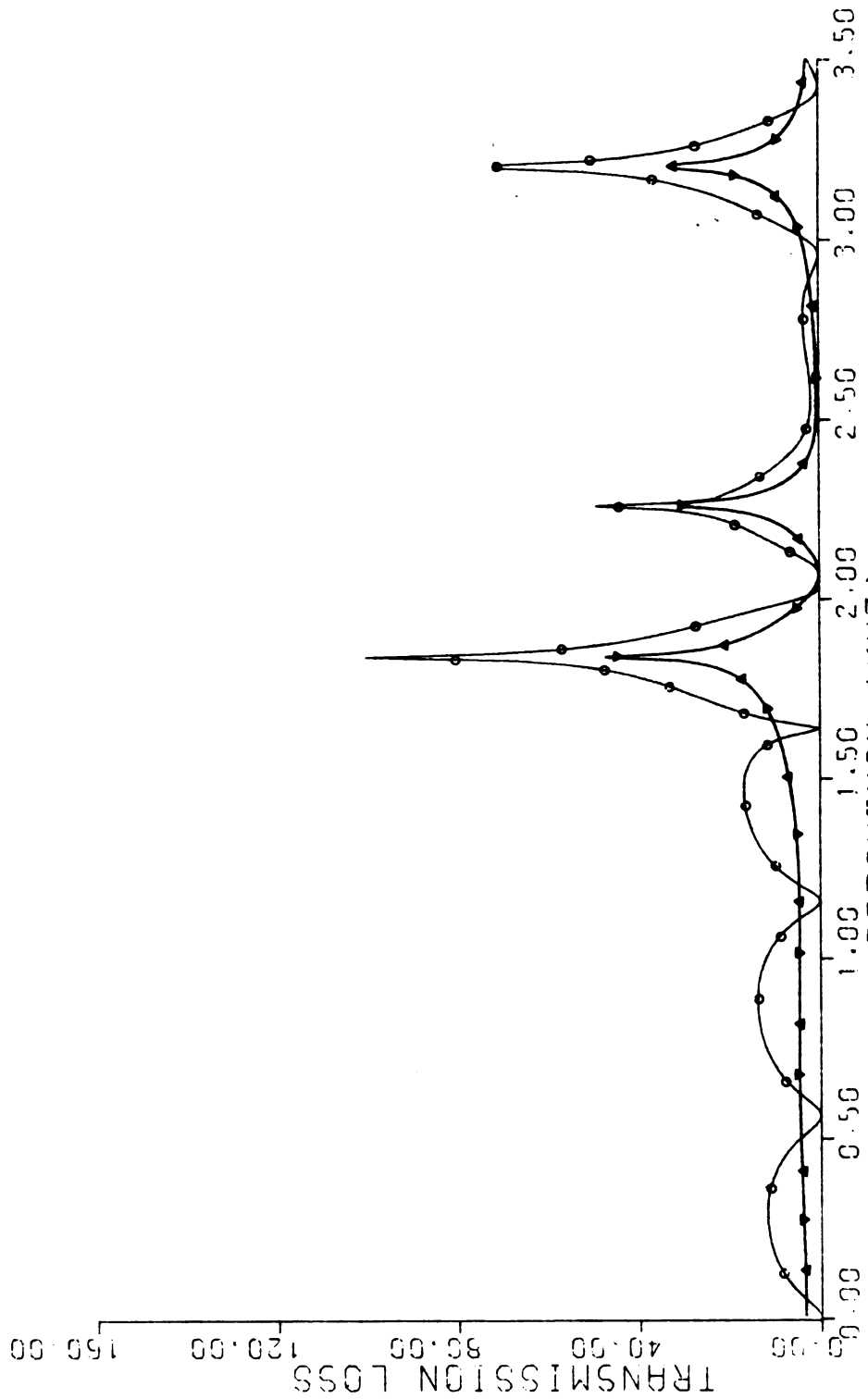

Figure 7. Plug muffler: $\ell_e = \ell_c = 6$ in, $\sigma_e = \sigma_c = .0481$; M = 0.

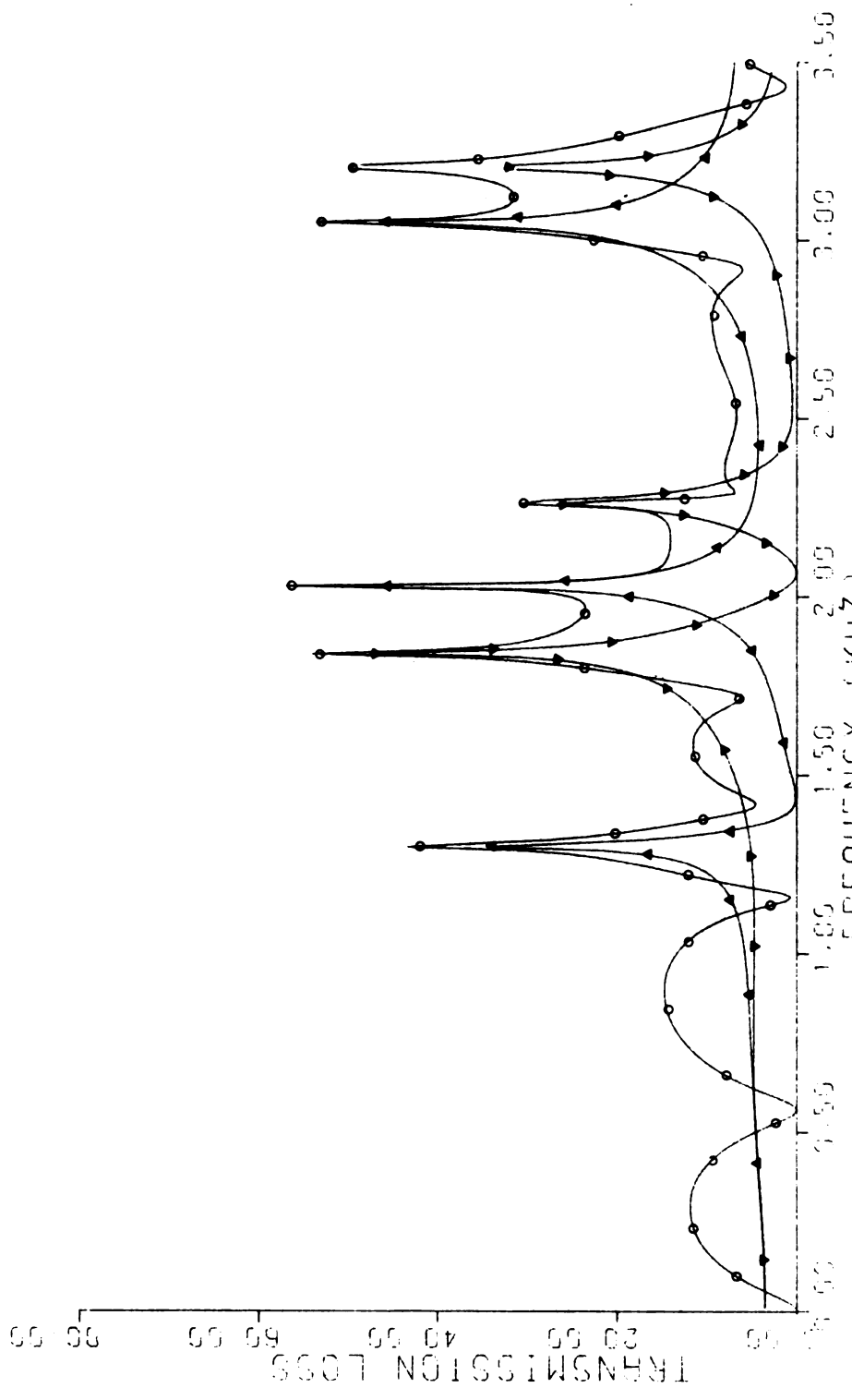

Figure 8. Plug muffler: $\ell_e = \ell_c = 6$ in, $\sigma_e = .02405$, $\sigma_c = .0481$; M = 0.

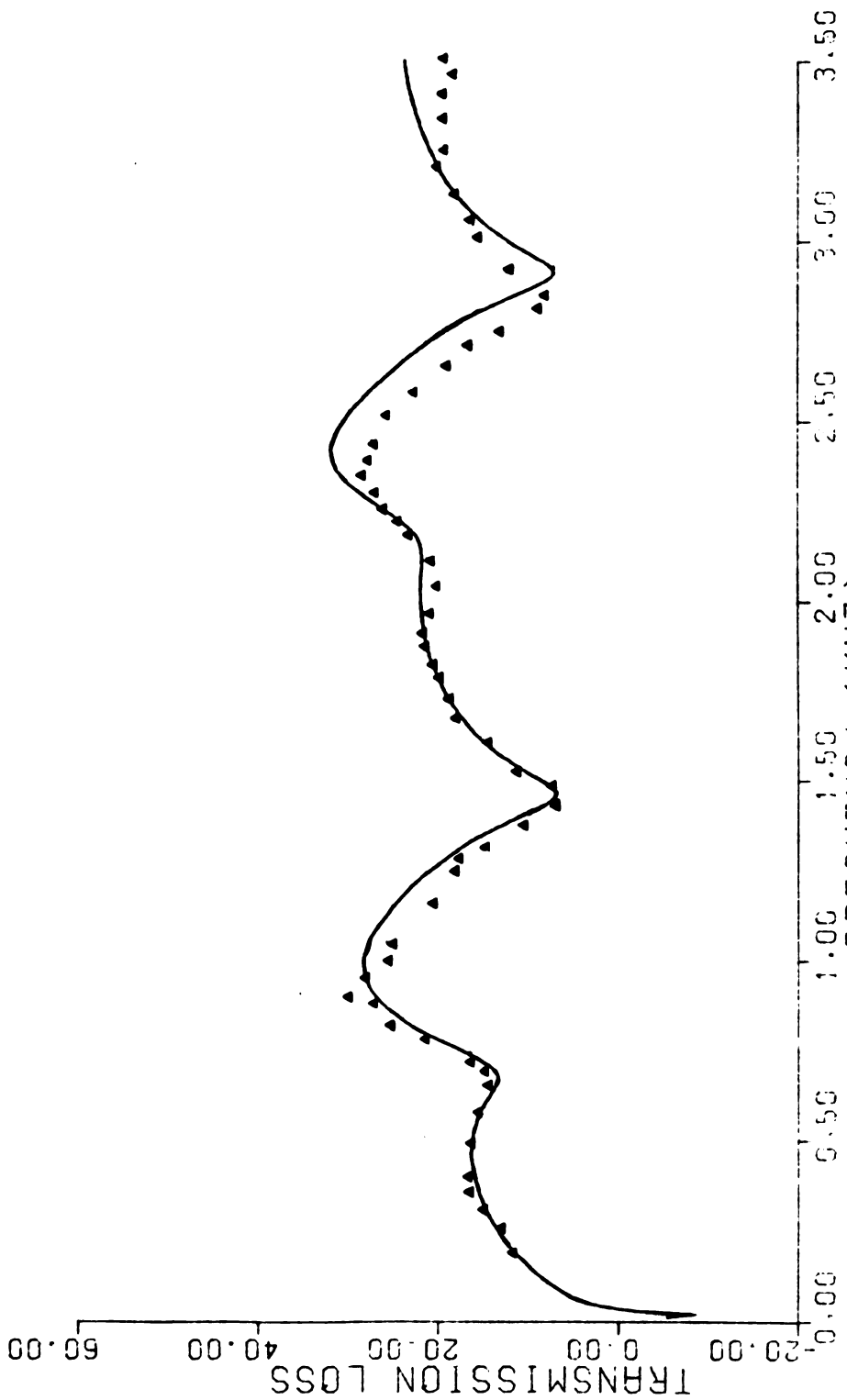

Figure 9. Center plug, 3.9% uniform porosity, M = .05. ▲ experimental data (74°C).

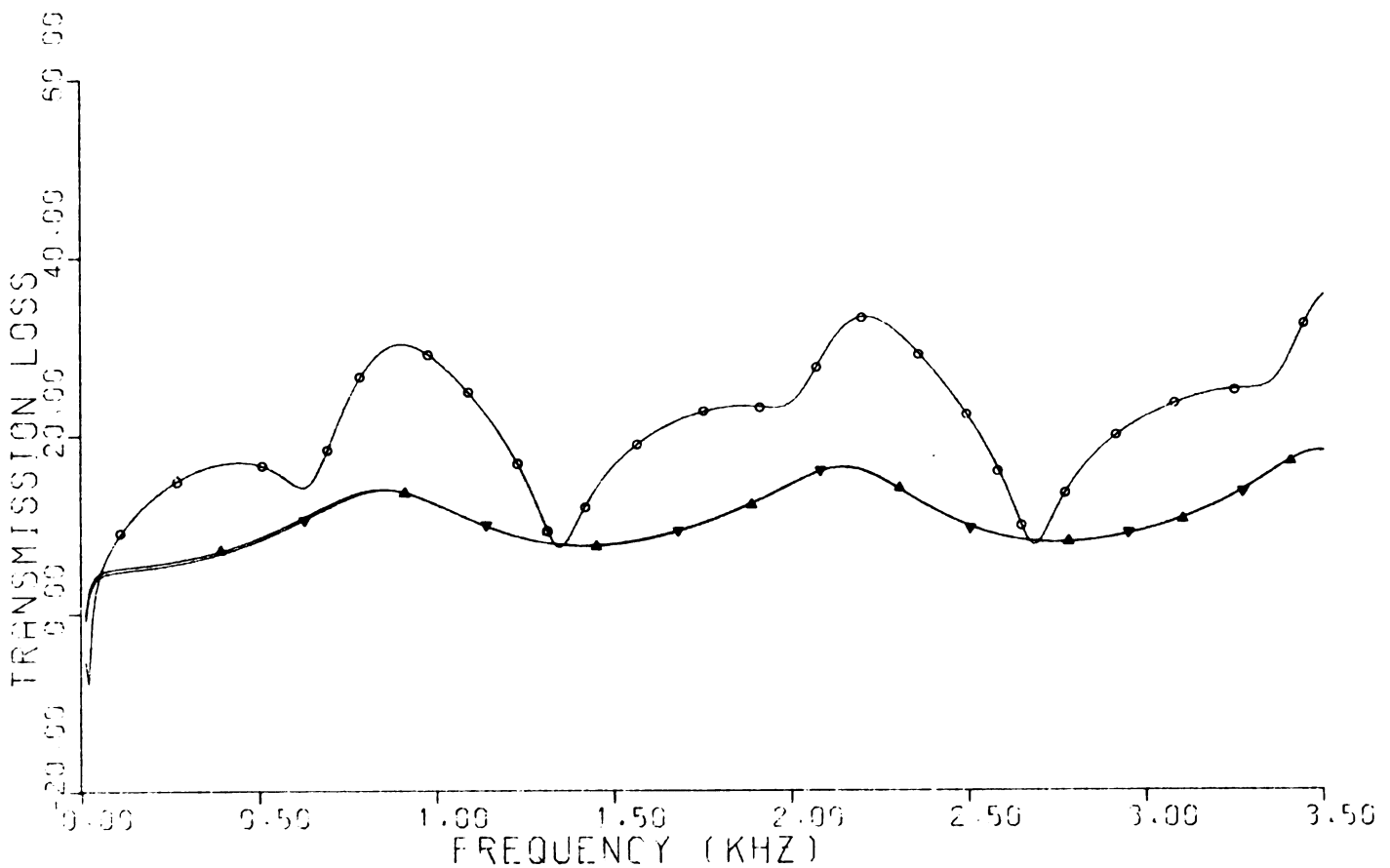

Figure 10. Center plug, 3.9% uniform porosity M = .05 (22°C).

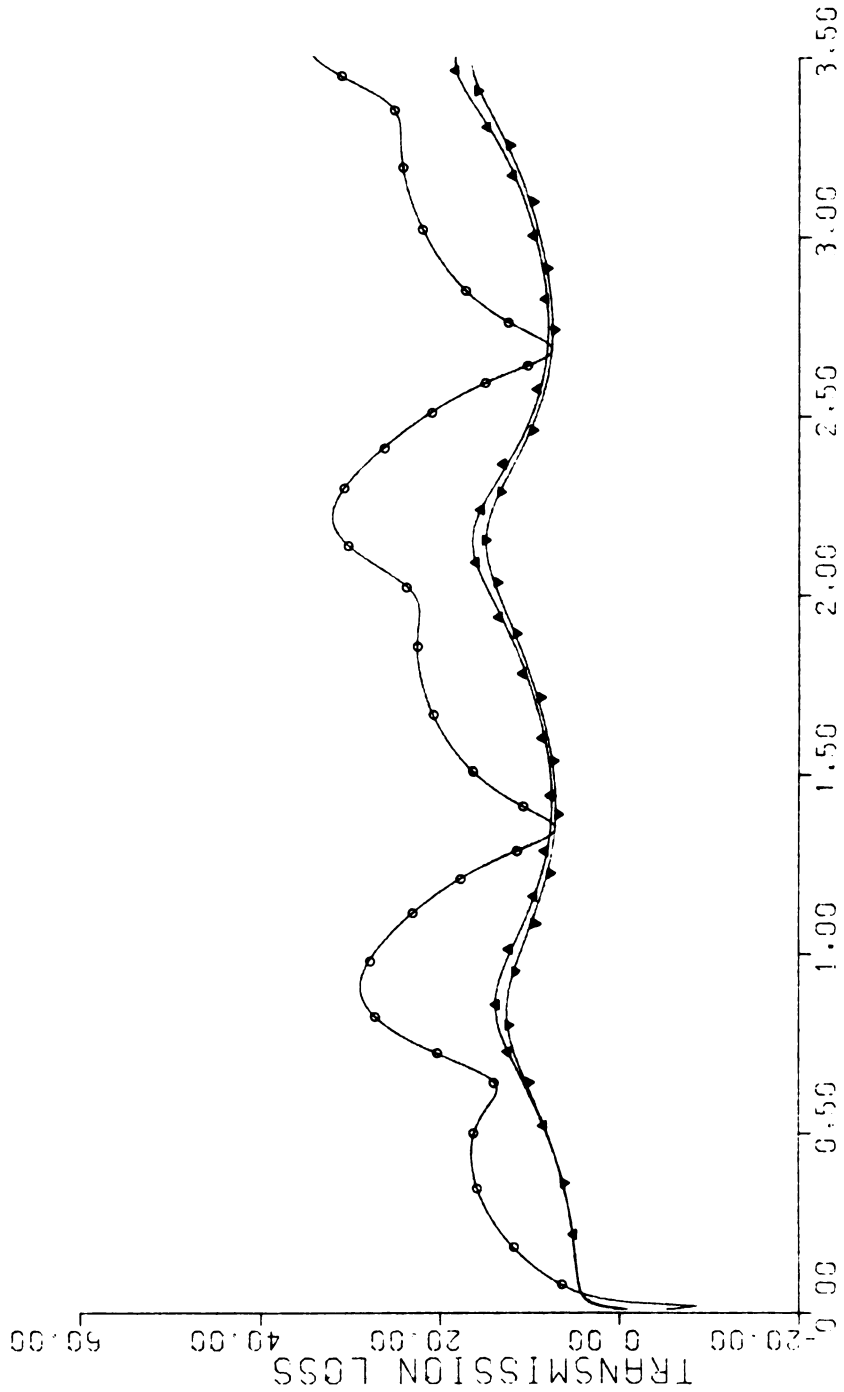

Figure 11. Center plug, different porosities, M = .05 σ_e = 3.9%; σ_c = 4.5%.

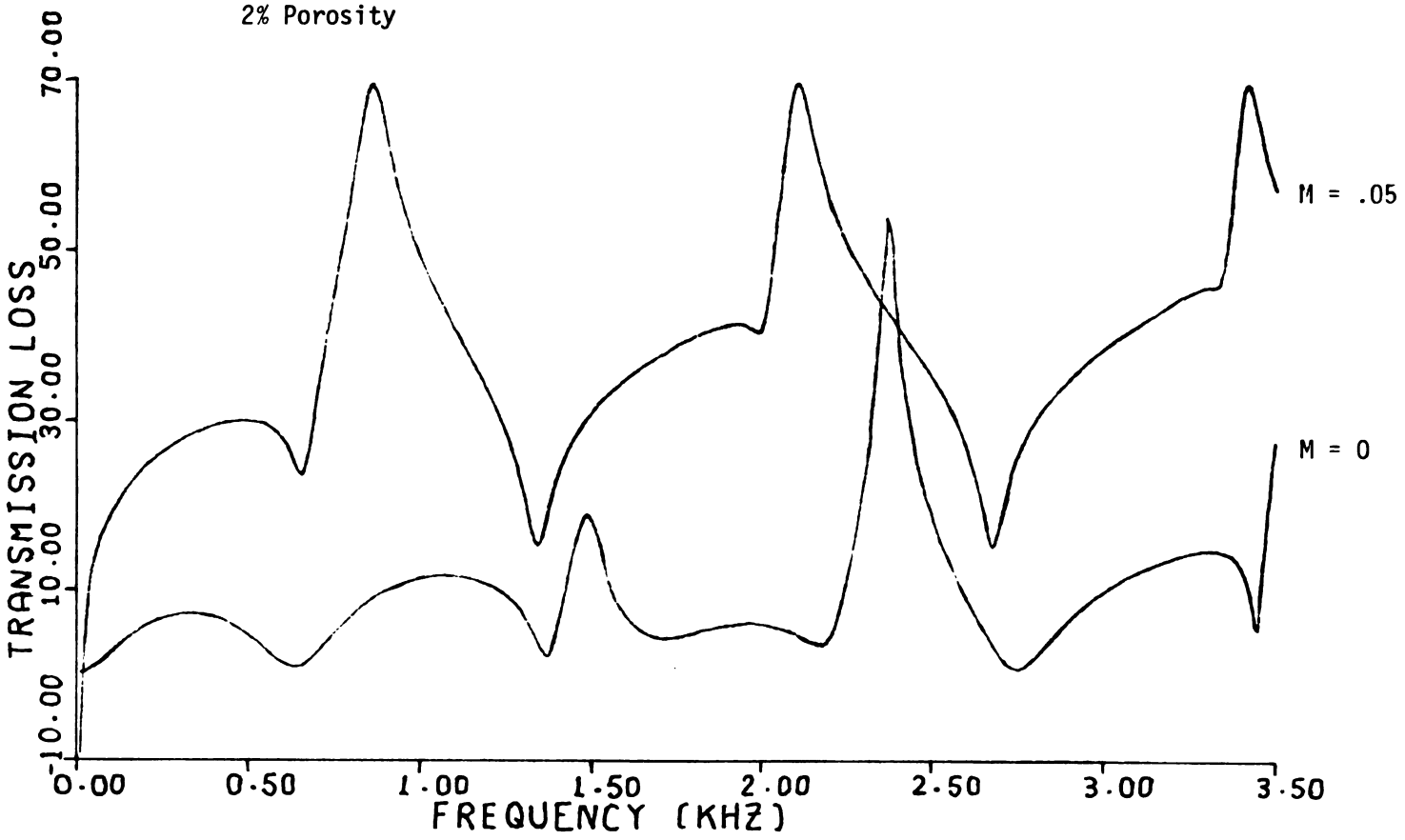

Figure 12. Comparison of transmission loss with M=0 and M=.05 for 2% open area on centered plug muffler.

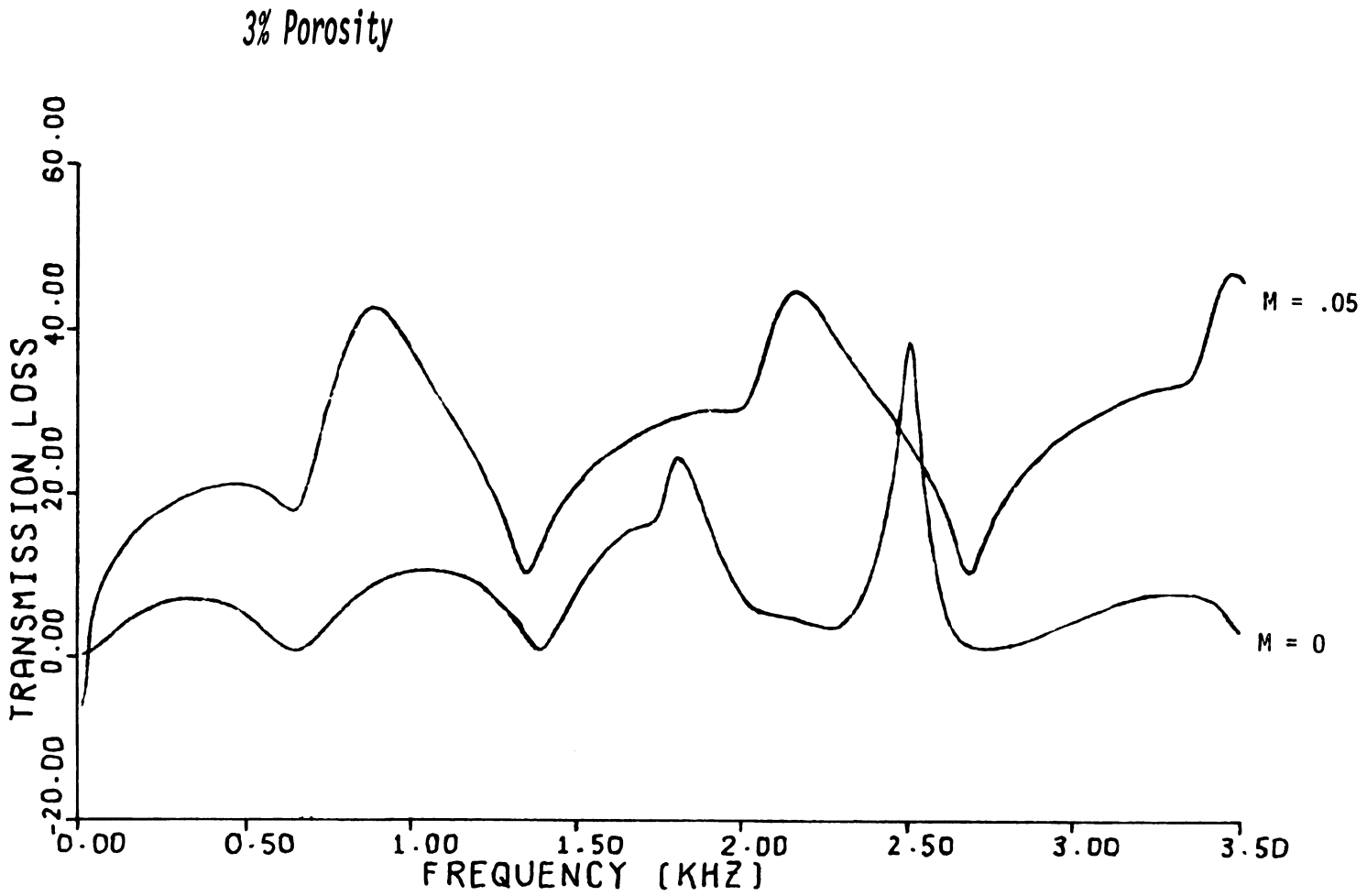

Figure 13. Comparison of transmission loss with M=0 and M=.05 for 3% open area on centered plug muffler.

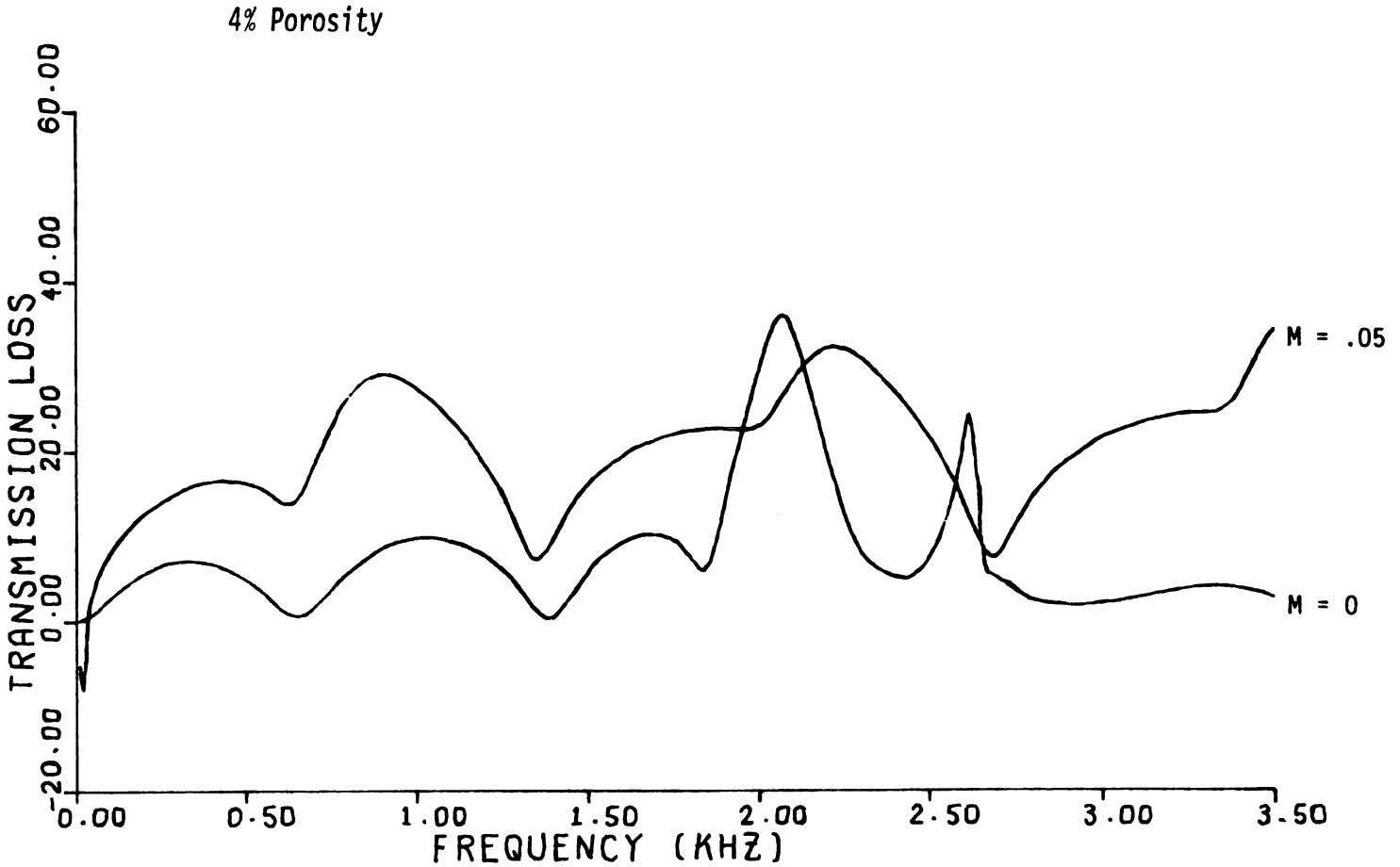

Figure 14. Comparison of transmission loss with M=0 and M=.05 for 4% open area on centered plug muffler.

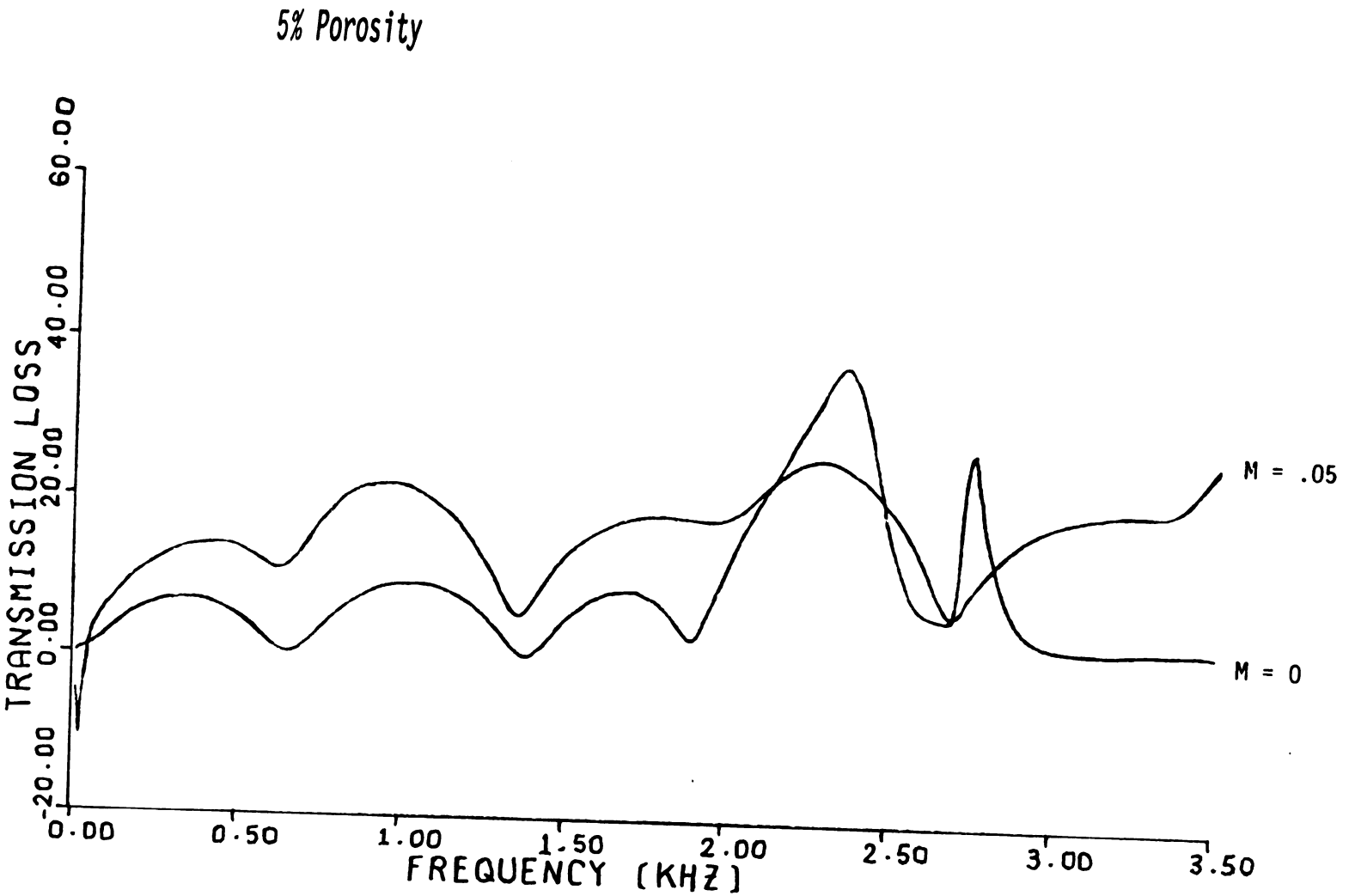

Figure 15. Comparison of transmission loss with M=0 and M=.05 for 5% open area on centered plug muffler.

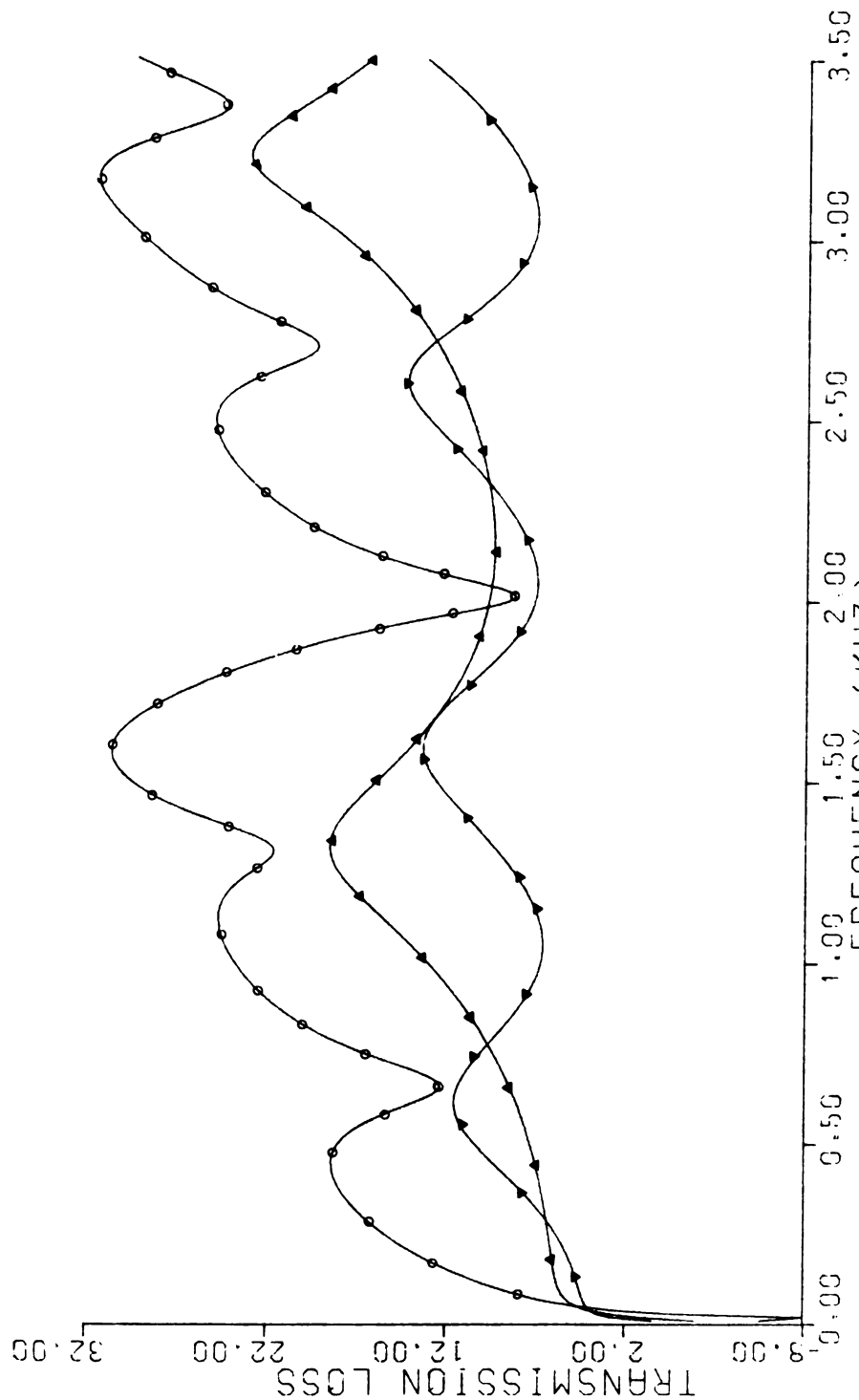

Figure 16. Offset plug ℓ_e = 85.7 mm; ℓ_c = 171.5 mm, 3.5% uniform porosity, M=.05.

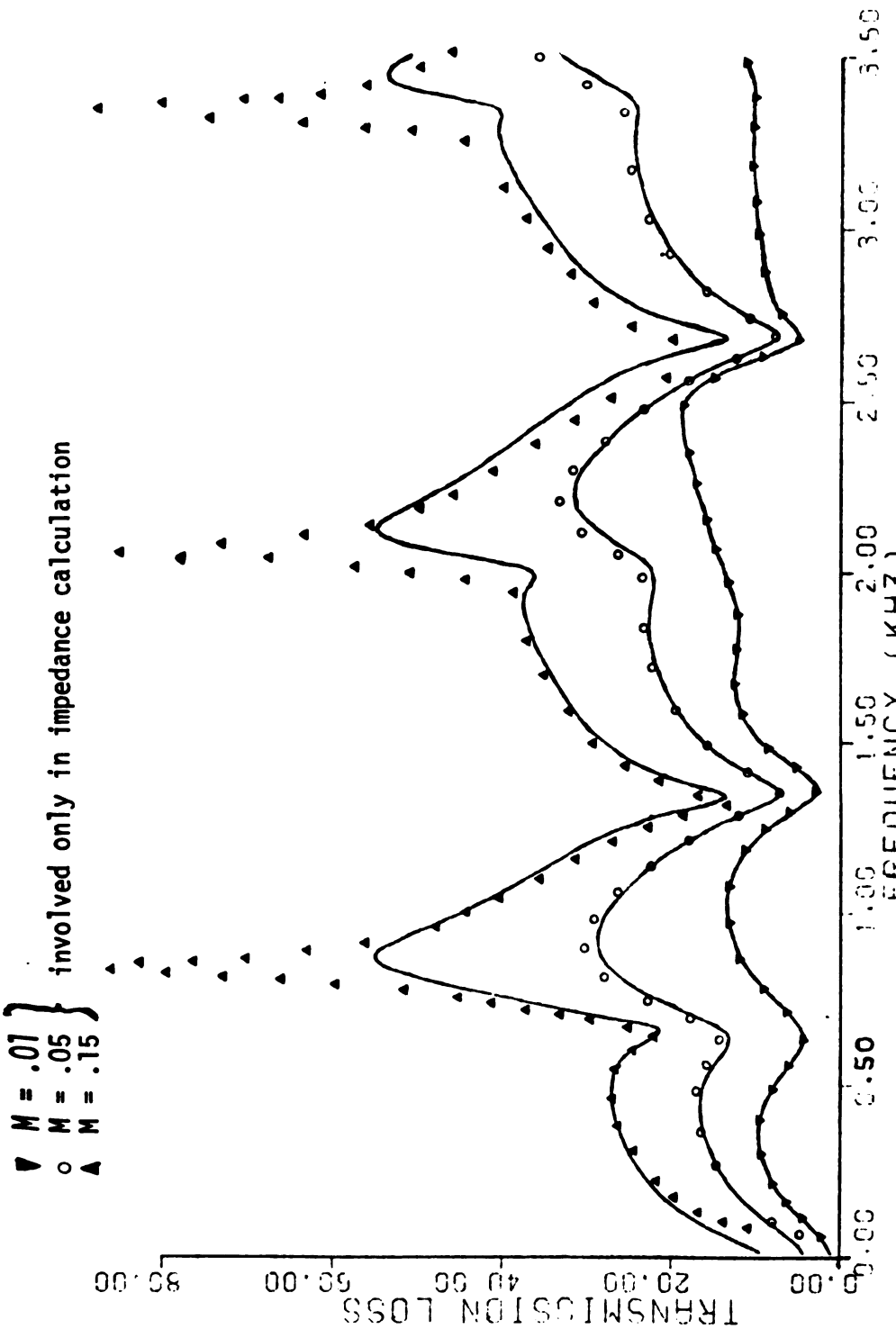

Figure 17. Predicted transmission loss of plug muffler.
—— include convective effects in calculation.

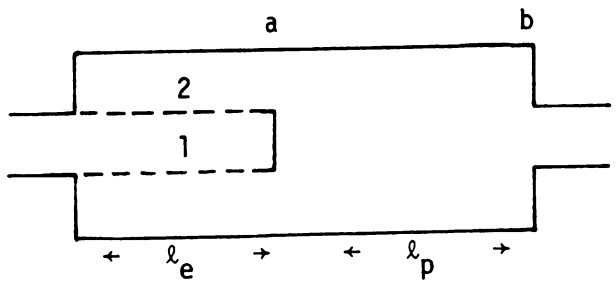

Figure 18. Configuration of a diffuser.

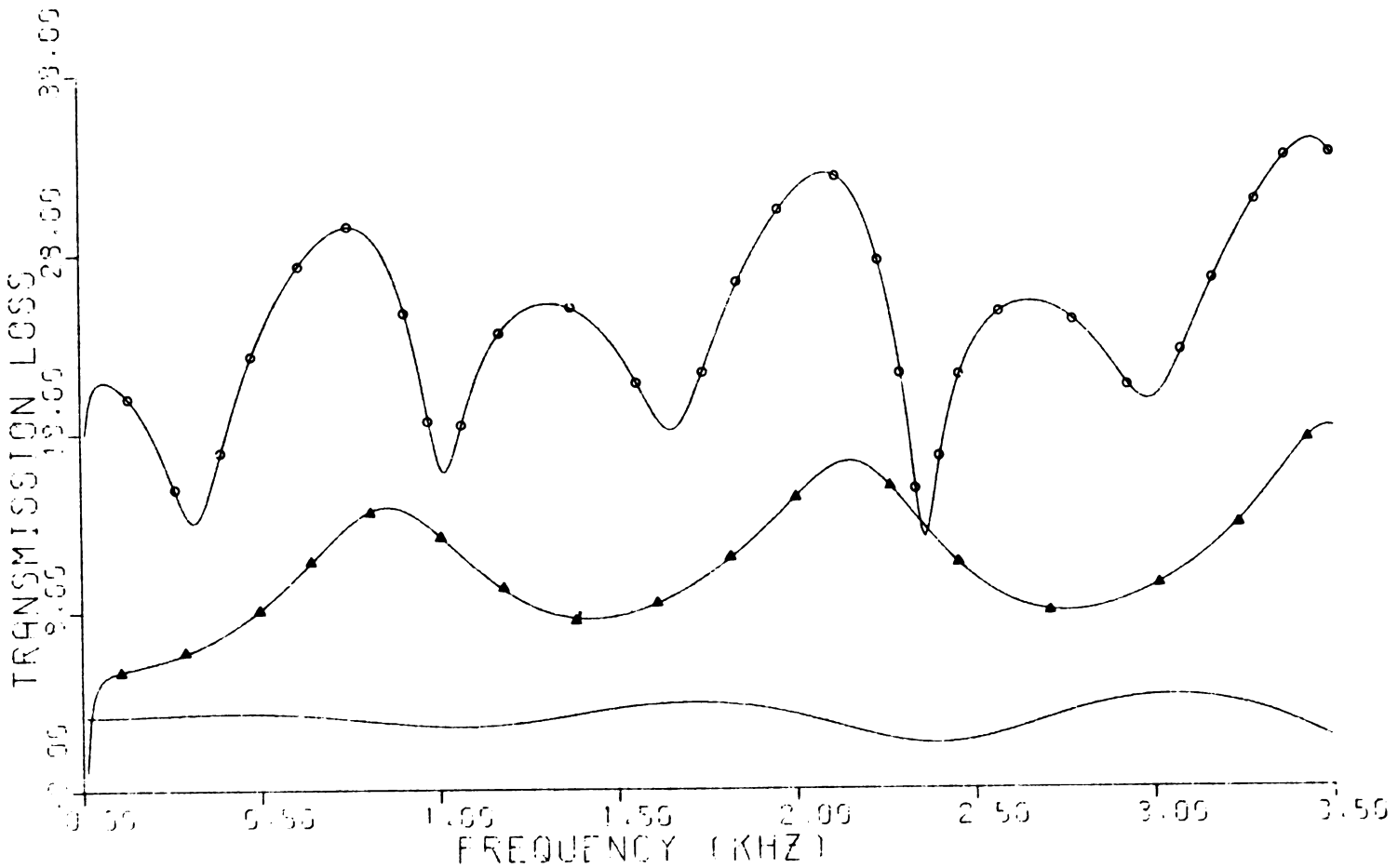

Figure 19. ℓ_e = 128.6 mm; ℓ_p = 128.6 mm; M = .05.

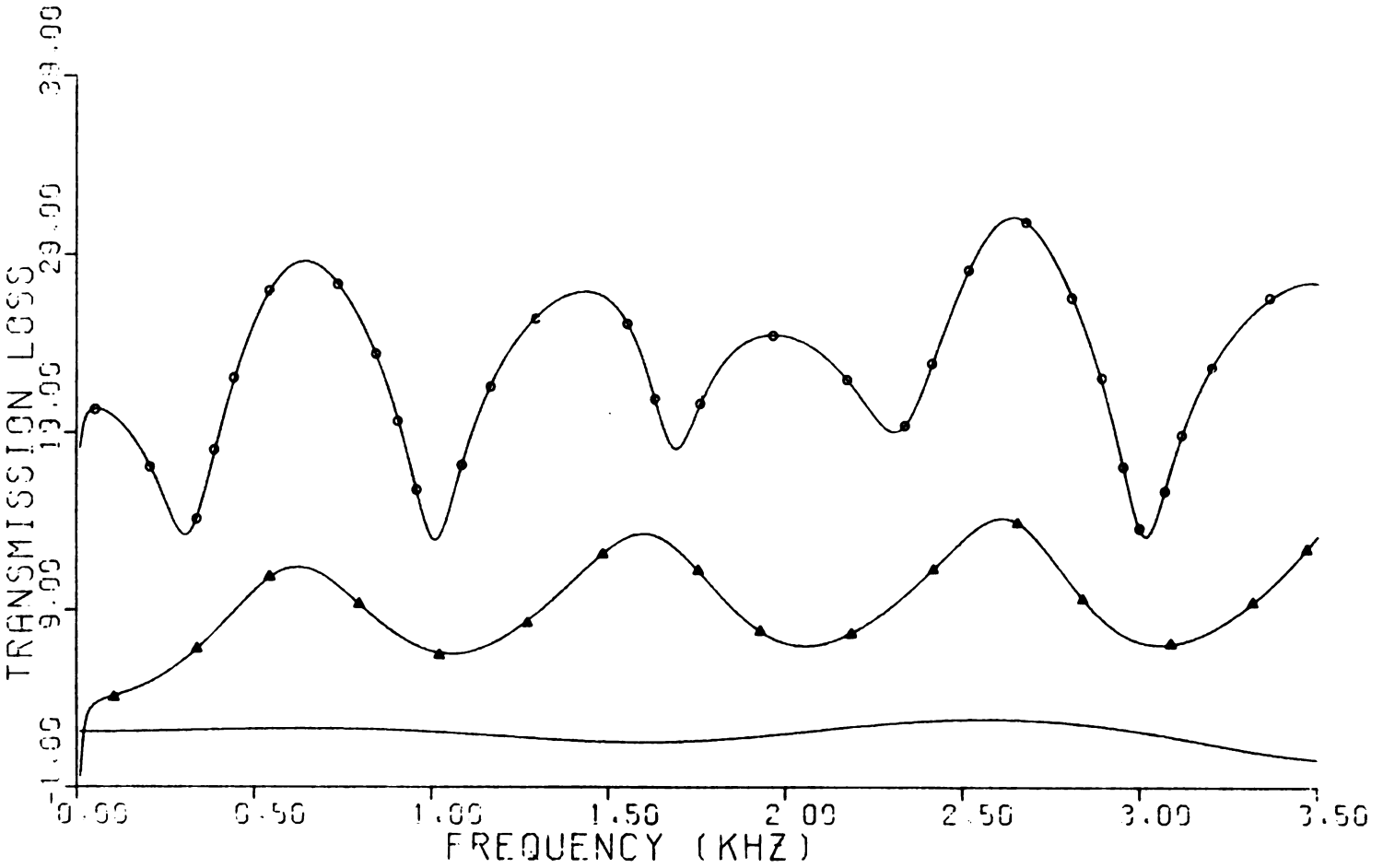

Figure 20. ℓ_e = 171.5 mm; ℓ_p = 85.7 mm; M = .05.

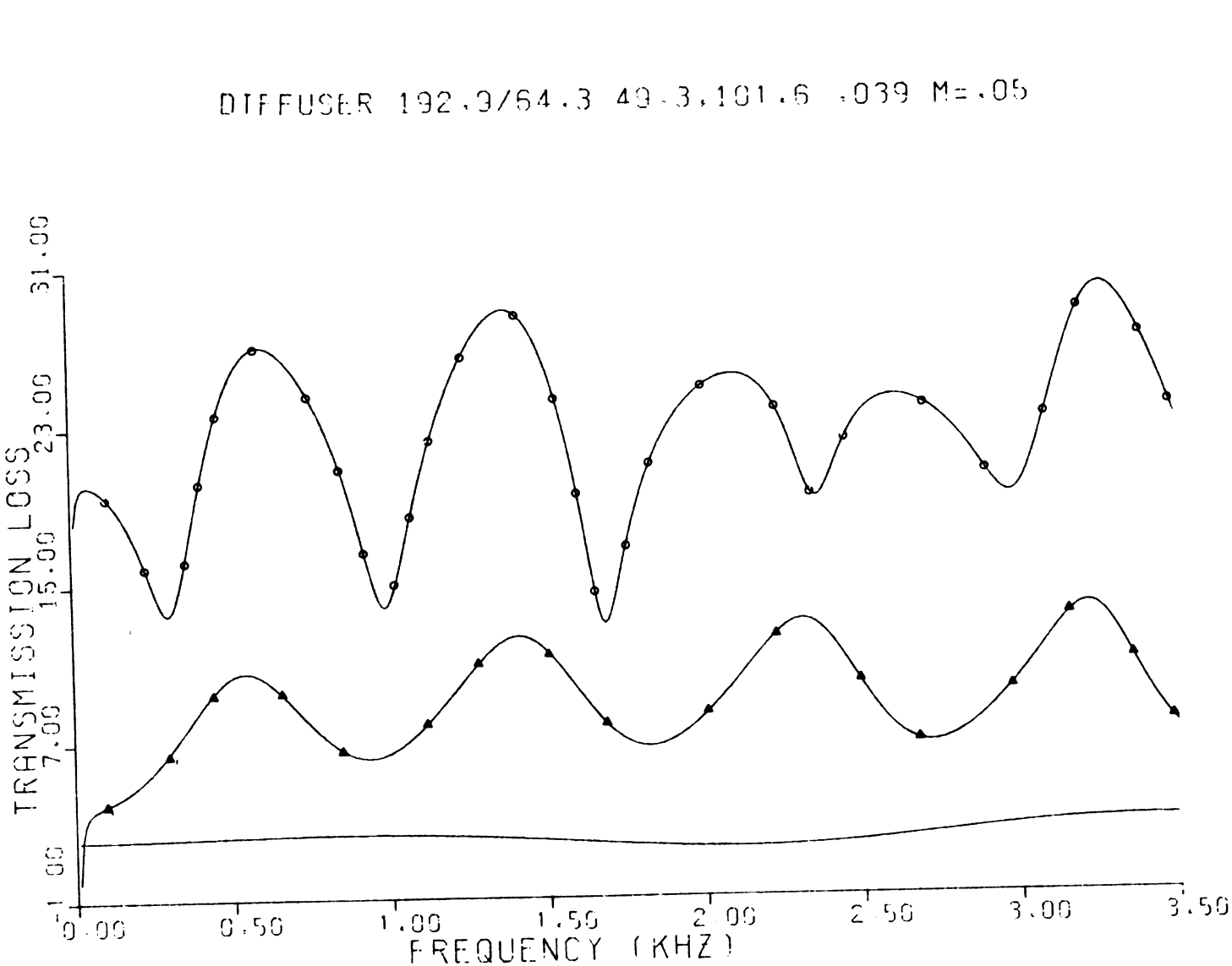

Figure 21. ℓ_e = 192.9 mm; ℓ_p = 64.3 mm; M = .05.

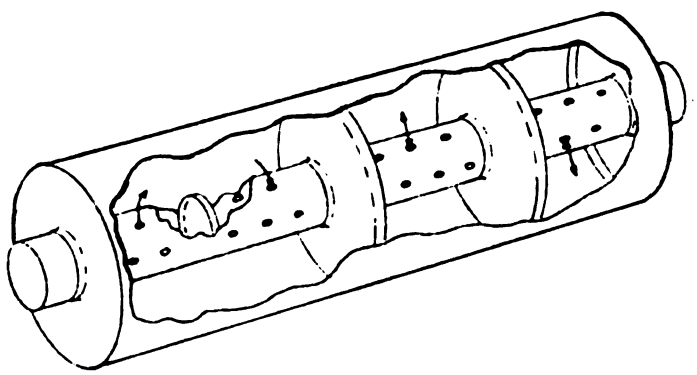

Figure 22. Muffler with several plug sections.

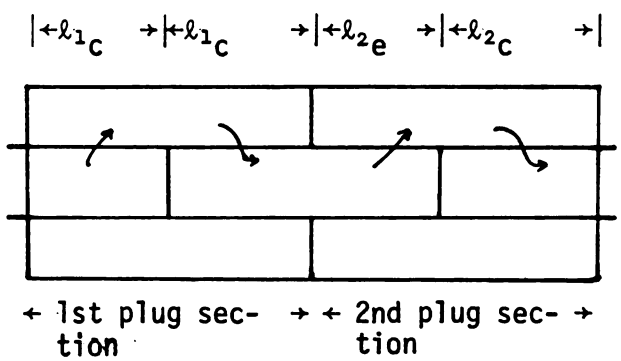

Figure 23. Schematic of muffler with two-plug sections.

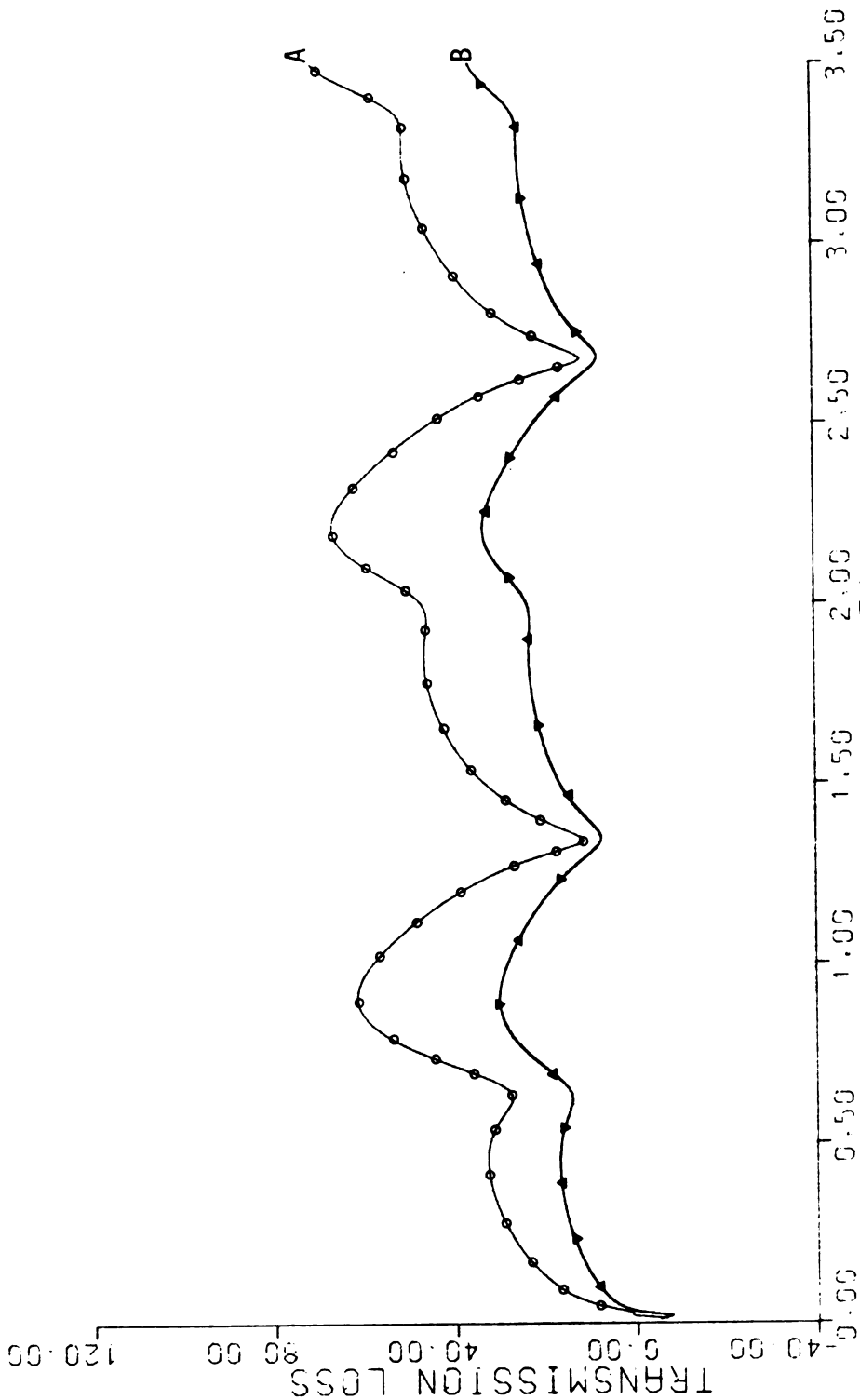

Figure 24. $\ell_{1e} = \ell_{1c} = \ell_{2e} = \ell_{2c} = 128.6$ mm; M = .05.

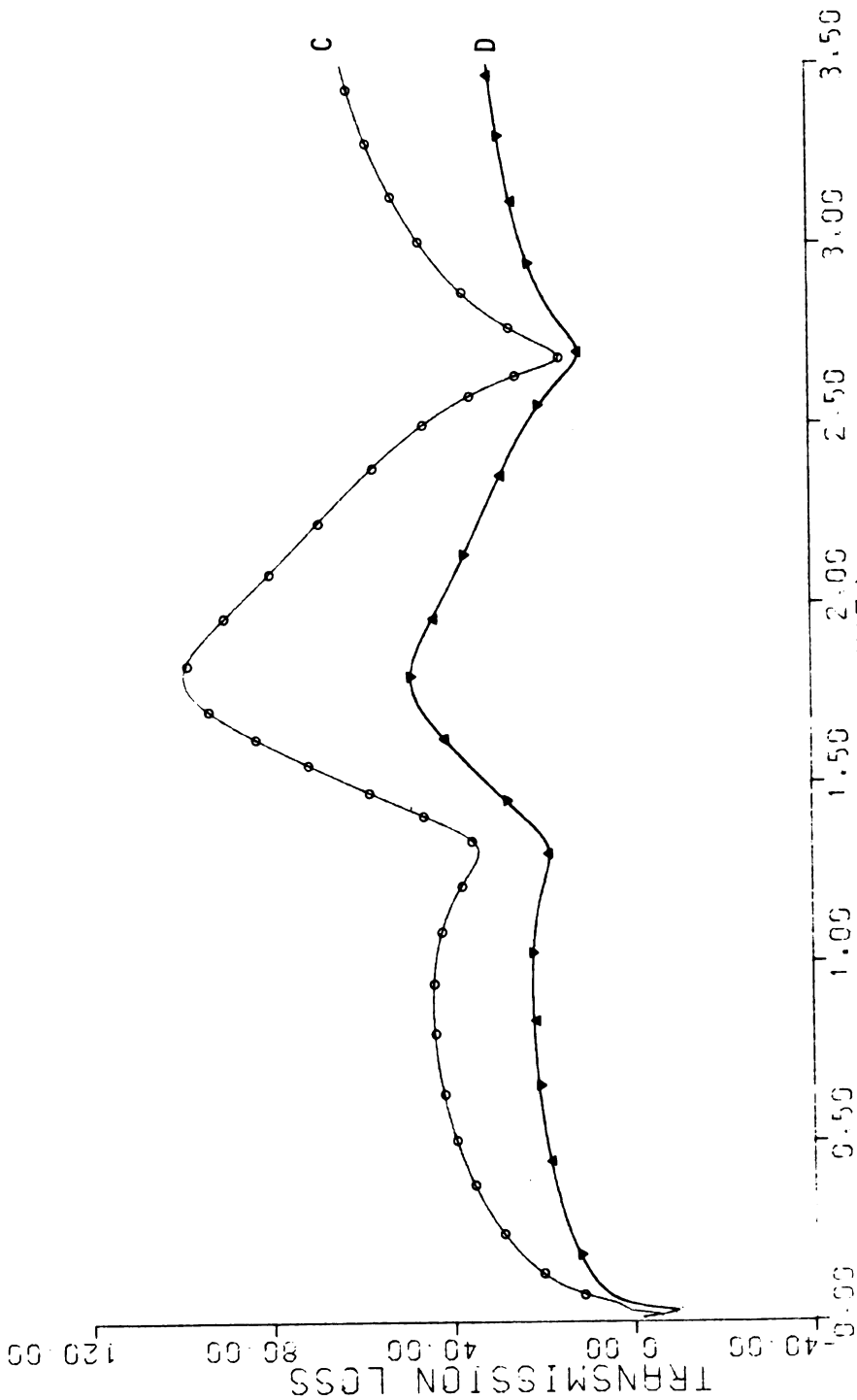

Figure 25. $\ell_{1e} = \ell_{1c} = \ell_{2e} = \ell_{2c} = 64.3$ mm; M = .05.

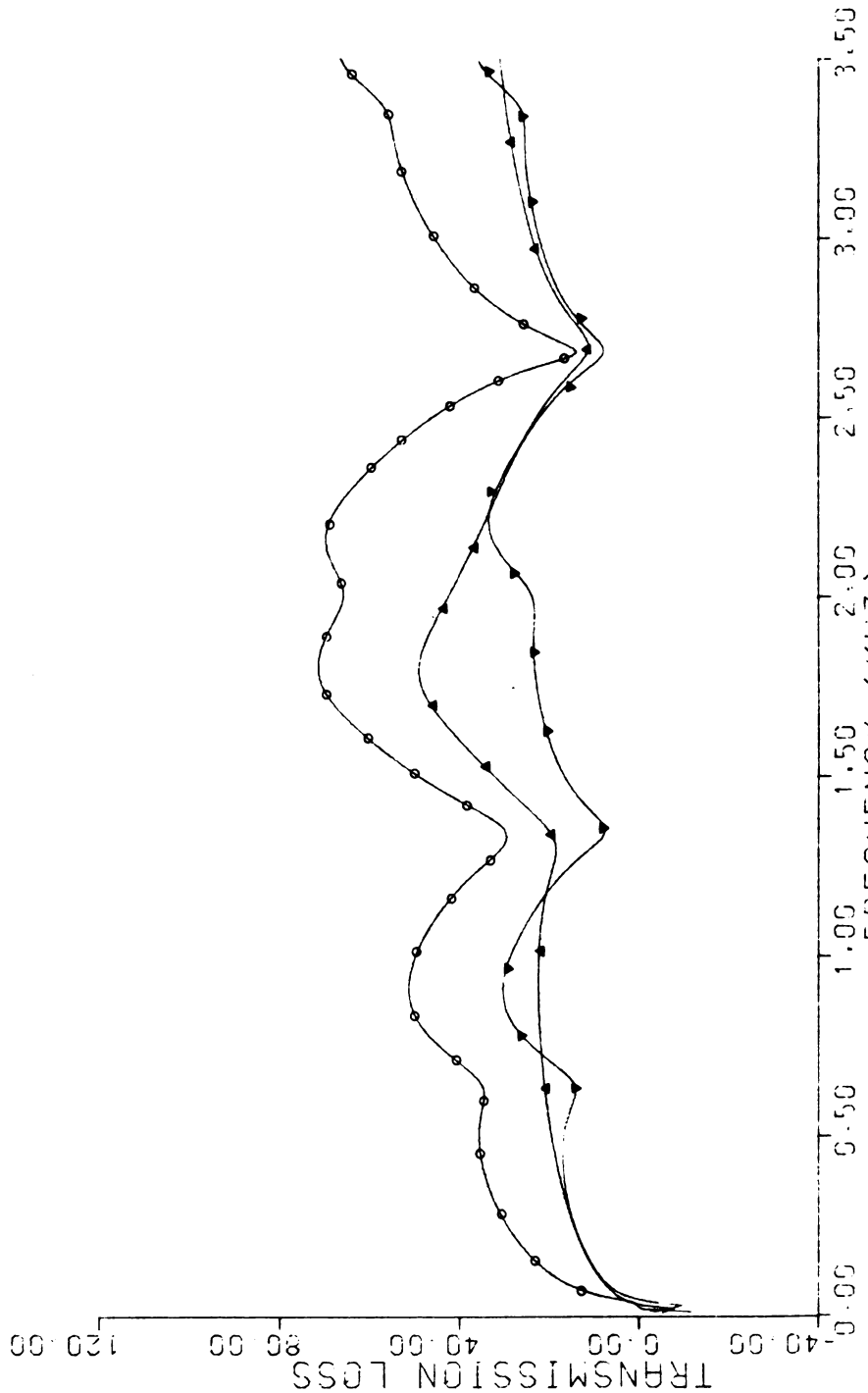

Figure 26. $\ell_{1e} = \ell_{1c} = 64.3$ mm; $\ell_{2e} = \ell_{2c} = 128.6$ mm; M = .05.

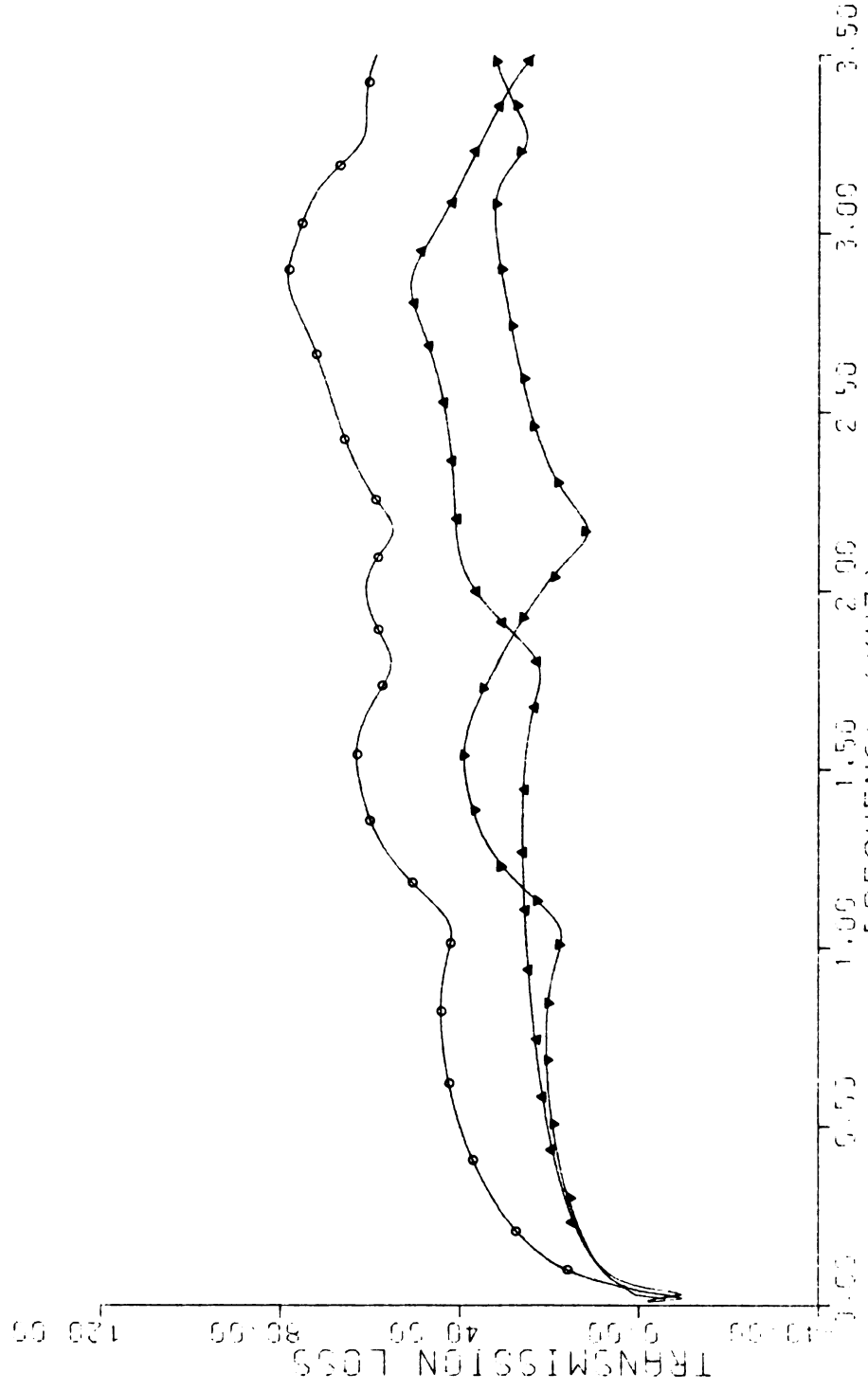

Figure 27. ℓ_{1_e} = 40 mm; ℓ_{1_c} = 56 mm; ℓ_{2_e} = 72 mm; ℓ_{2_c} = 88 mm; M = .05.

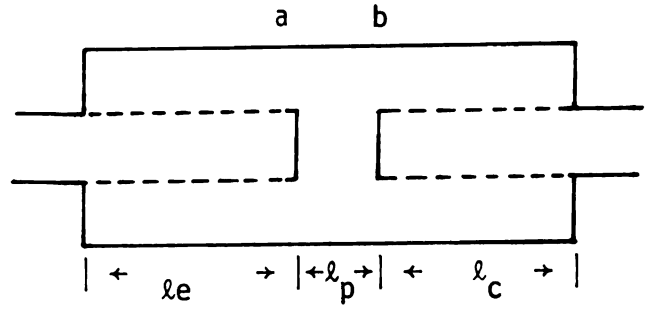

Figure 28. Configuration of a muffler with an empty space between two crossflow elements.

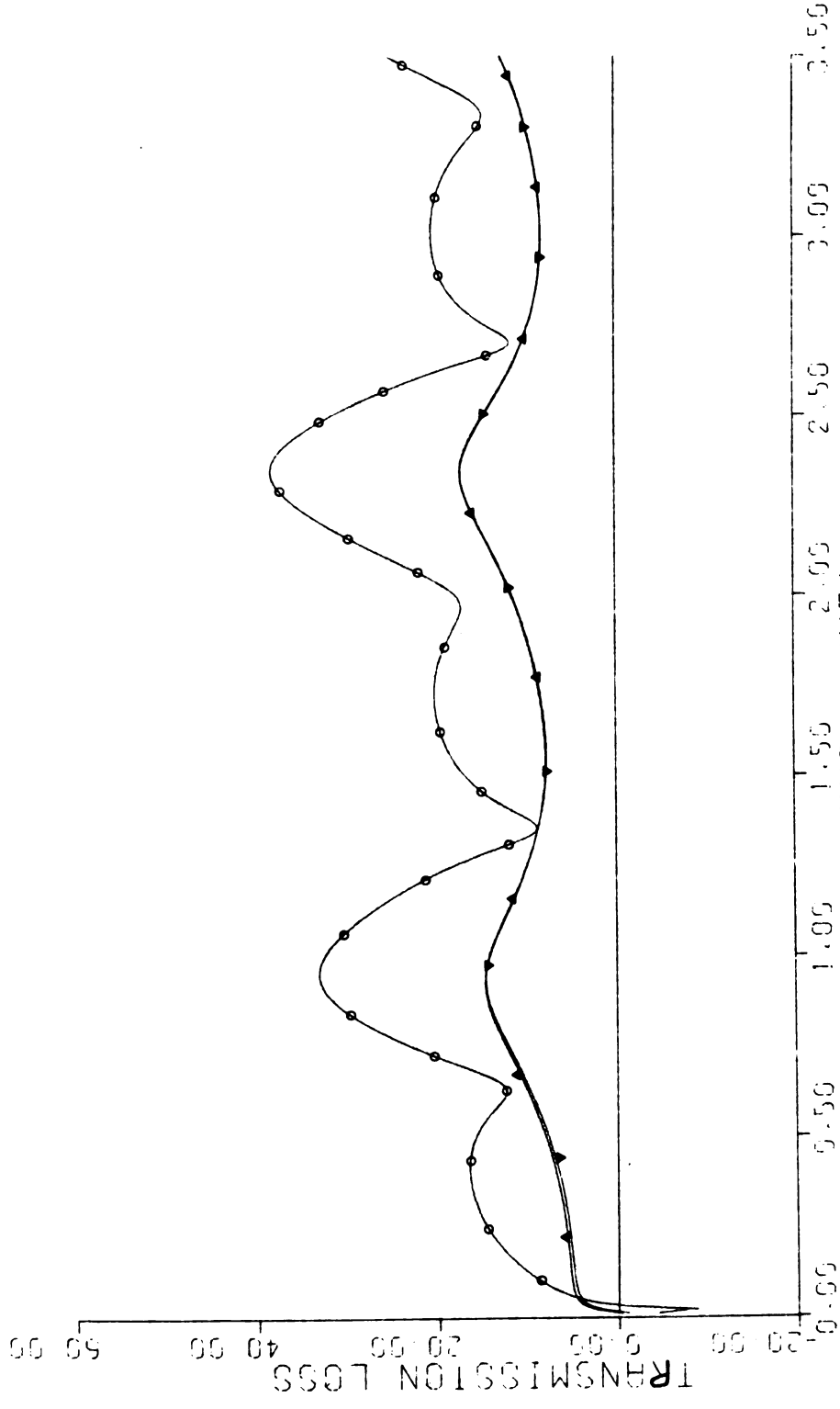

Figure 29. ℓ_e = 117.88; ℓ_p = 21.43 mm; ℓ_c = 117.88 mm; M = .05.

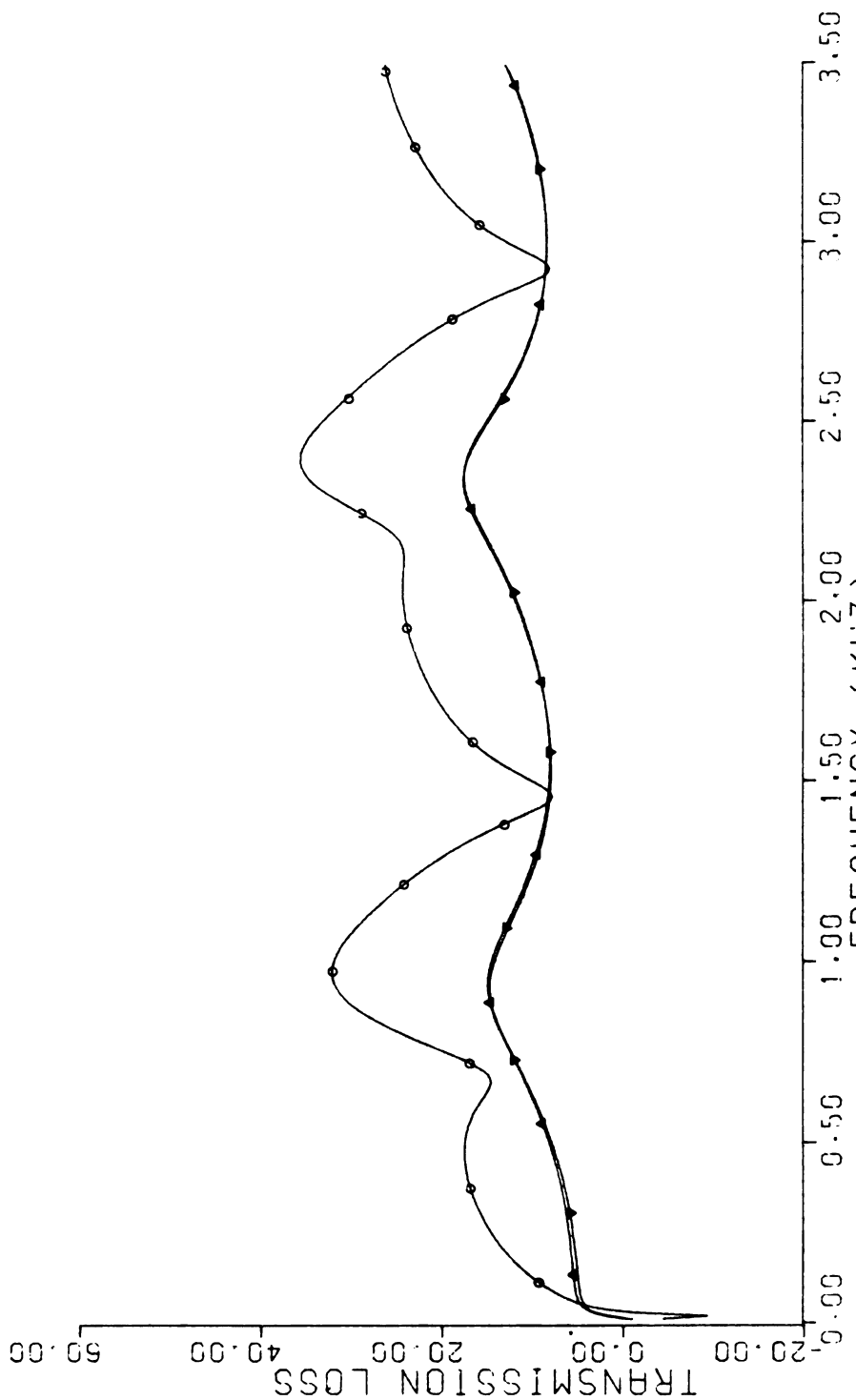

Figure 30. Plug muffler: ℓ_e = 117.88 mm; ℓ_c = 117.88 mm.; M = .05.

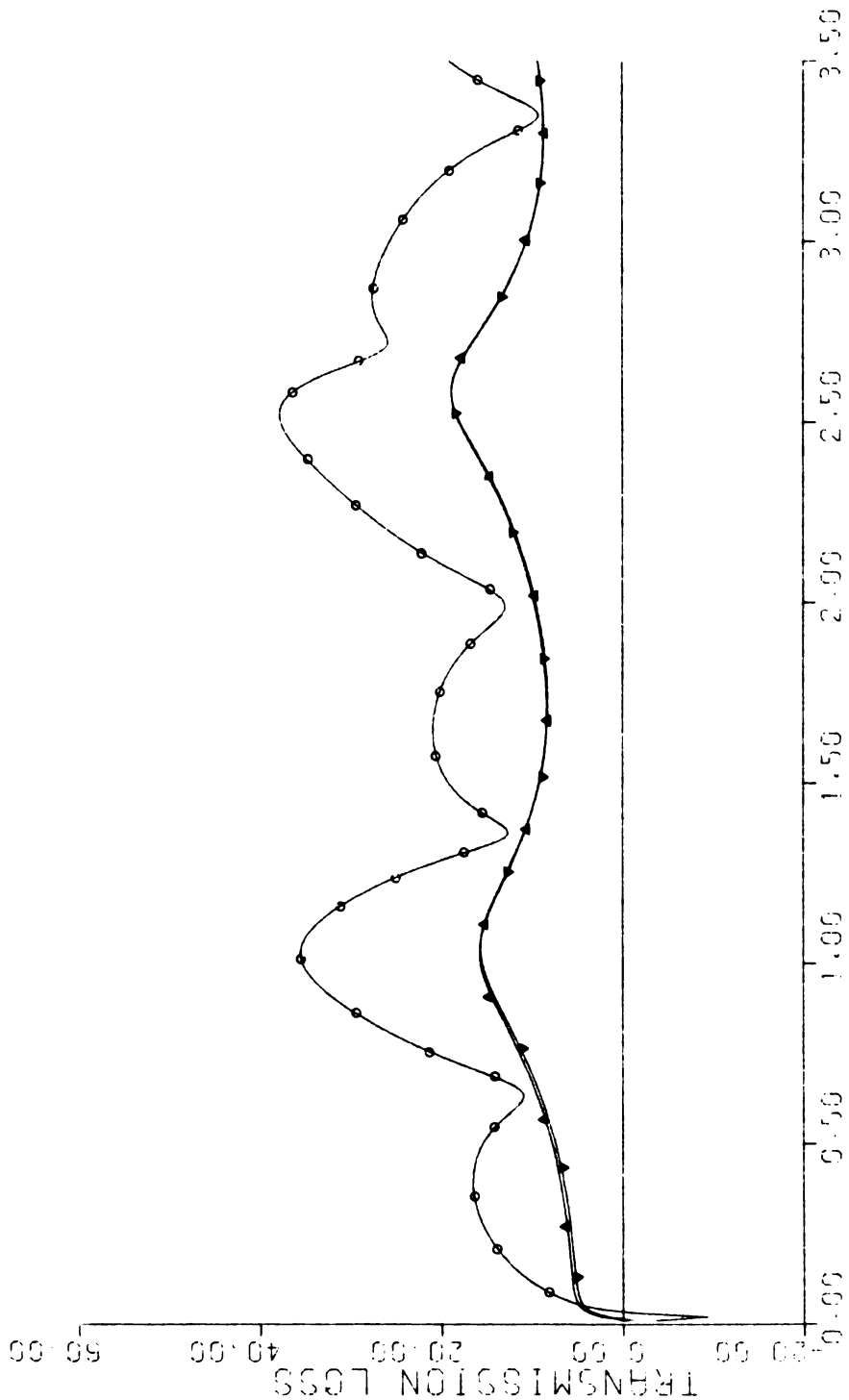

Figure 31. ℓ_e = 107.17 mm; ℓ_p = 42.87 mm; ℓ_c = 107.17 mm; M = .05.

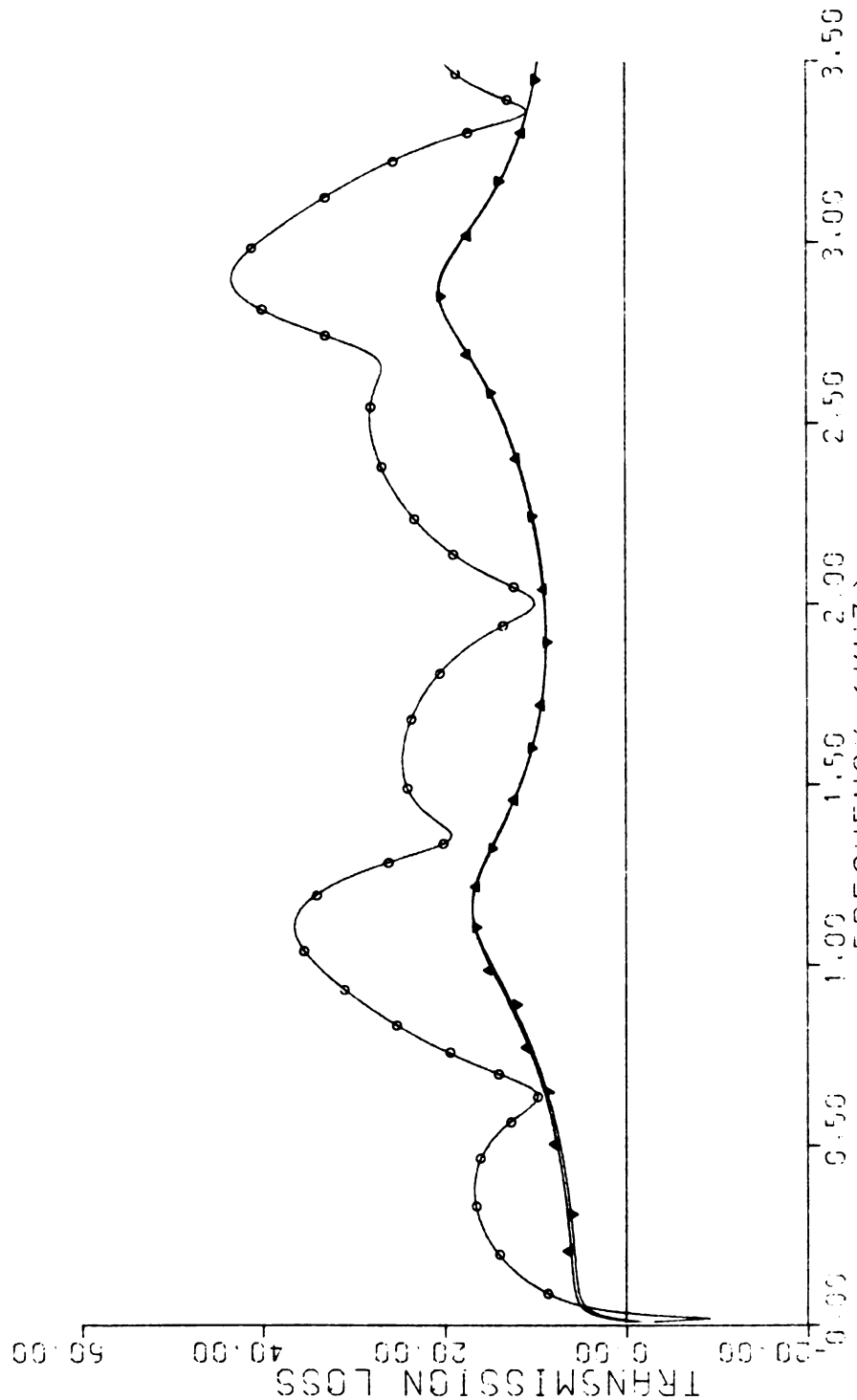

Figure 32. ℓ_e = 96.46 mm; ℓ_p = 64.29 mm; ℓ_c = 96.46 mm. ; M=.05.

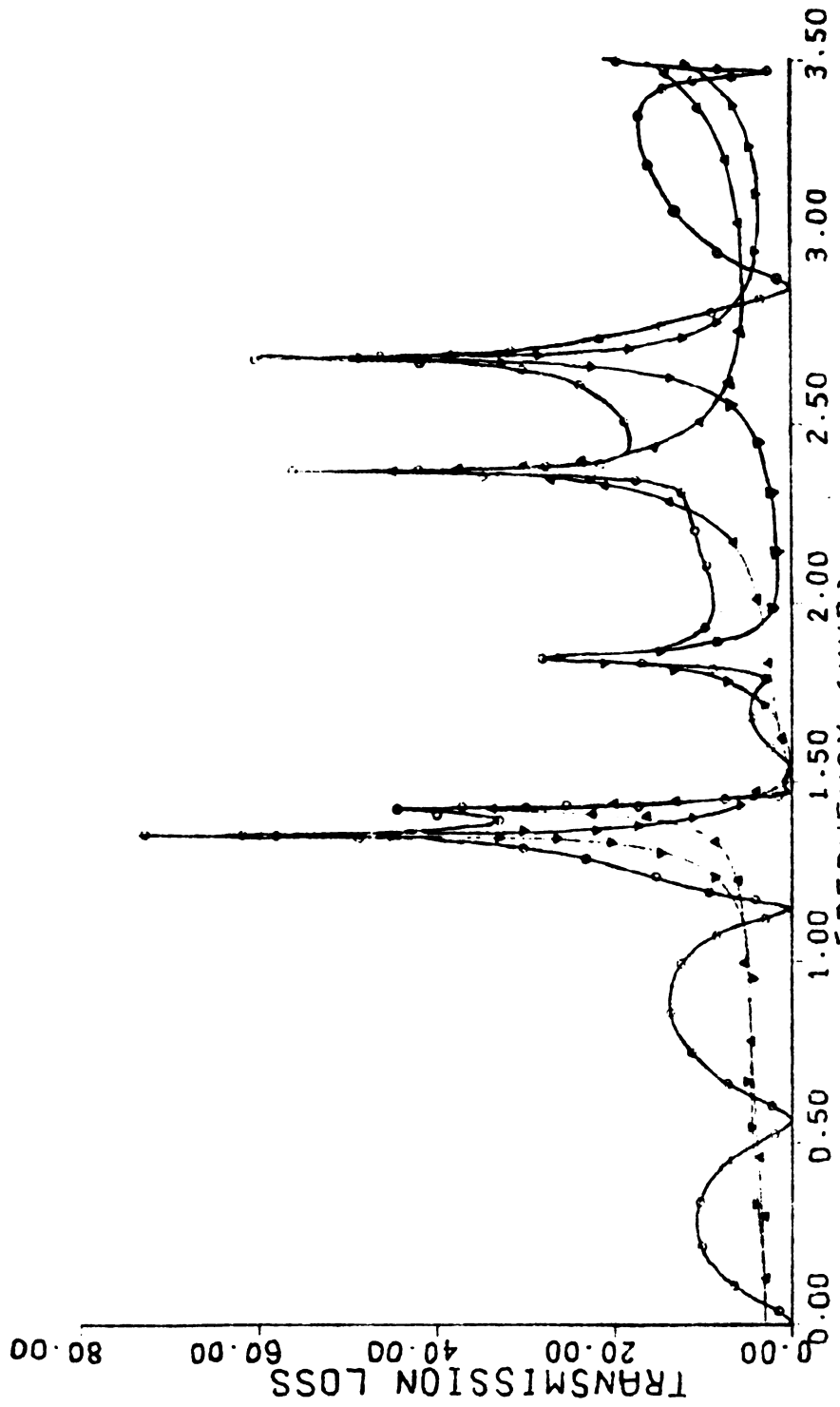

Figure 33. Transmission loss curve for uniform porosity plug muffler with different lengths before and after.
ℓ_e = 5 in; σ_e = .049 d_1 = 2.125 in; d_2 = 5.56 in
ℓ_c = 7 in; σ_c = .049 Δ = .245 in; M = 0

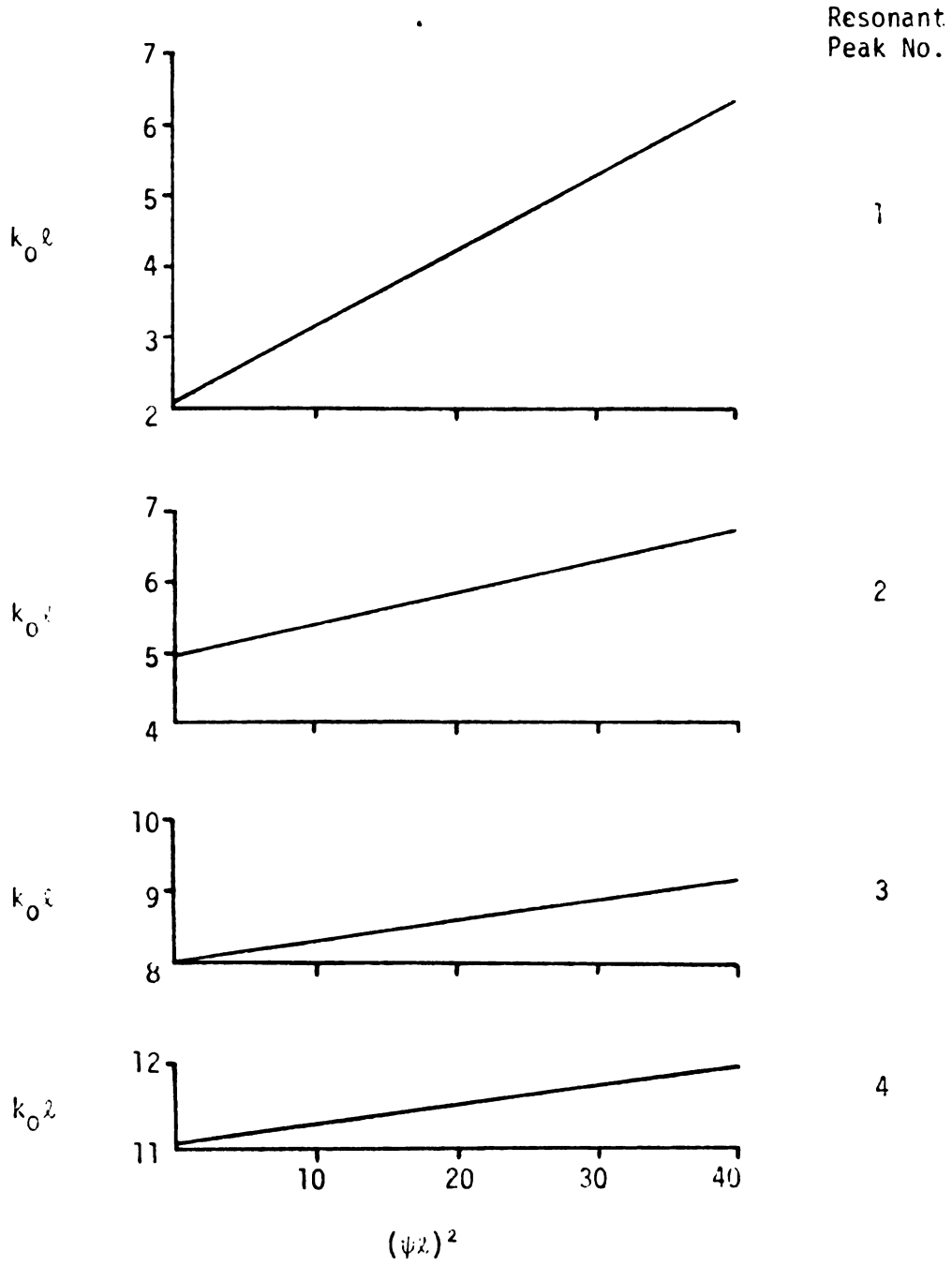

Figure 34. Straight line correlations between resonance frequencies of crossflow elements and the dimensionless group $(\psi\ell)^2 = \frac{4\sigma}{d_1\Delta} \frac{\ell^2}{(1-r^2)}$

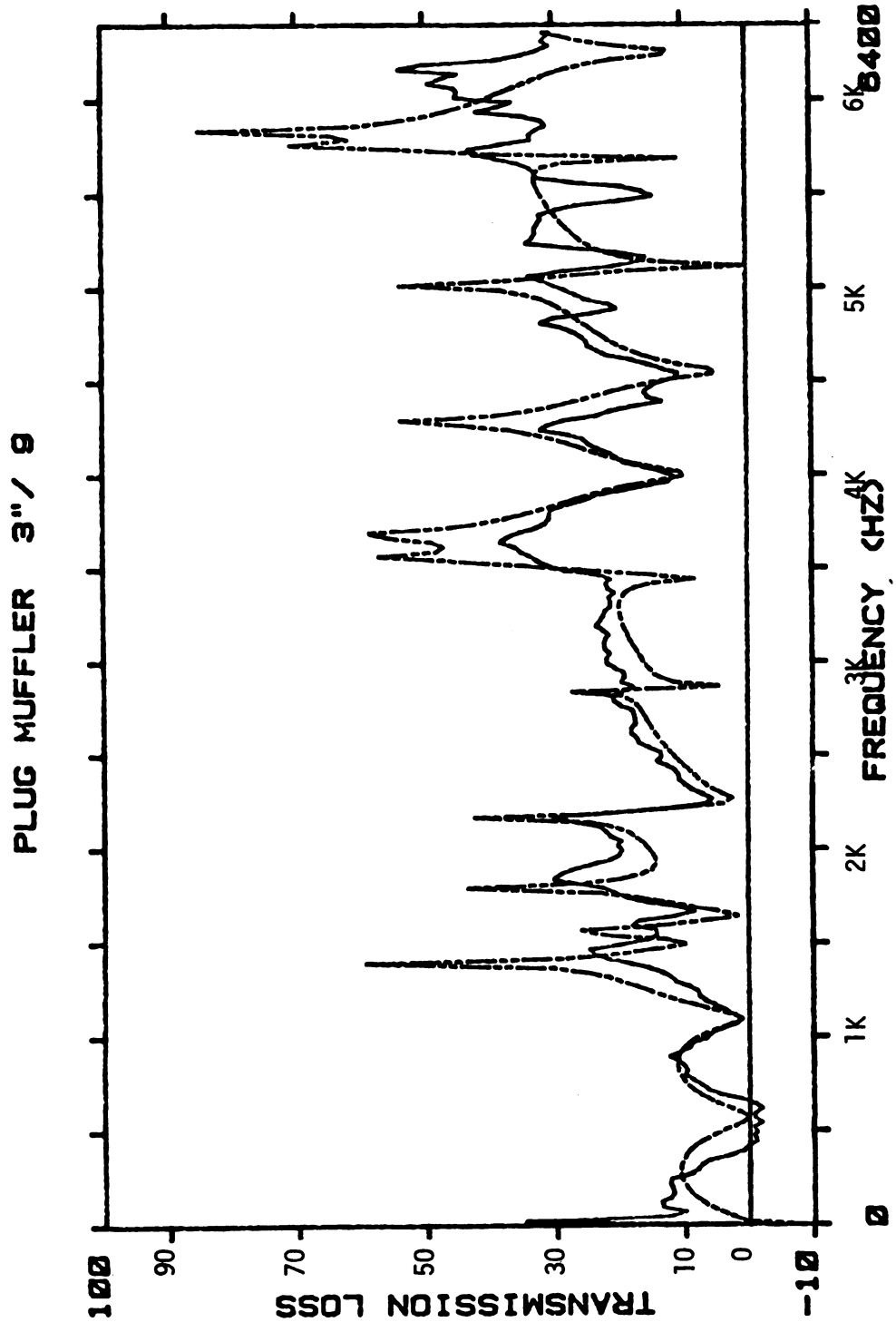

Figure 35. Plug muffler: ℓ_e = 3 in; ℓ_c = 9 in; $\sigma_e = \sigma_c$ = .049; M = 0.
——— experimental, - - - - - predicted.

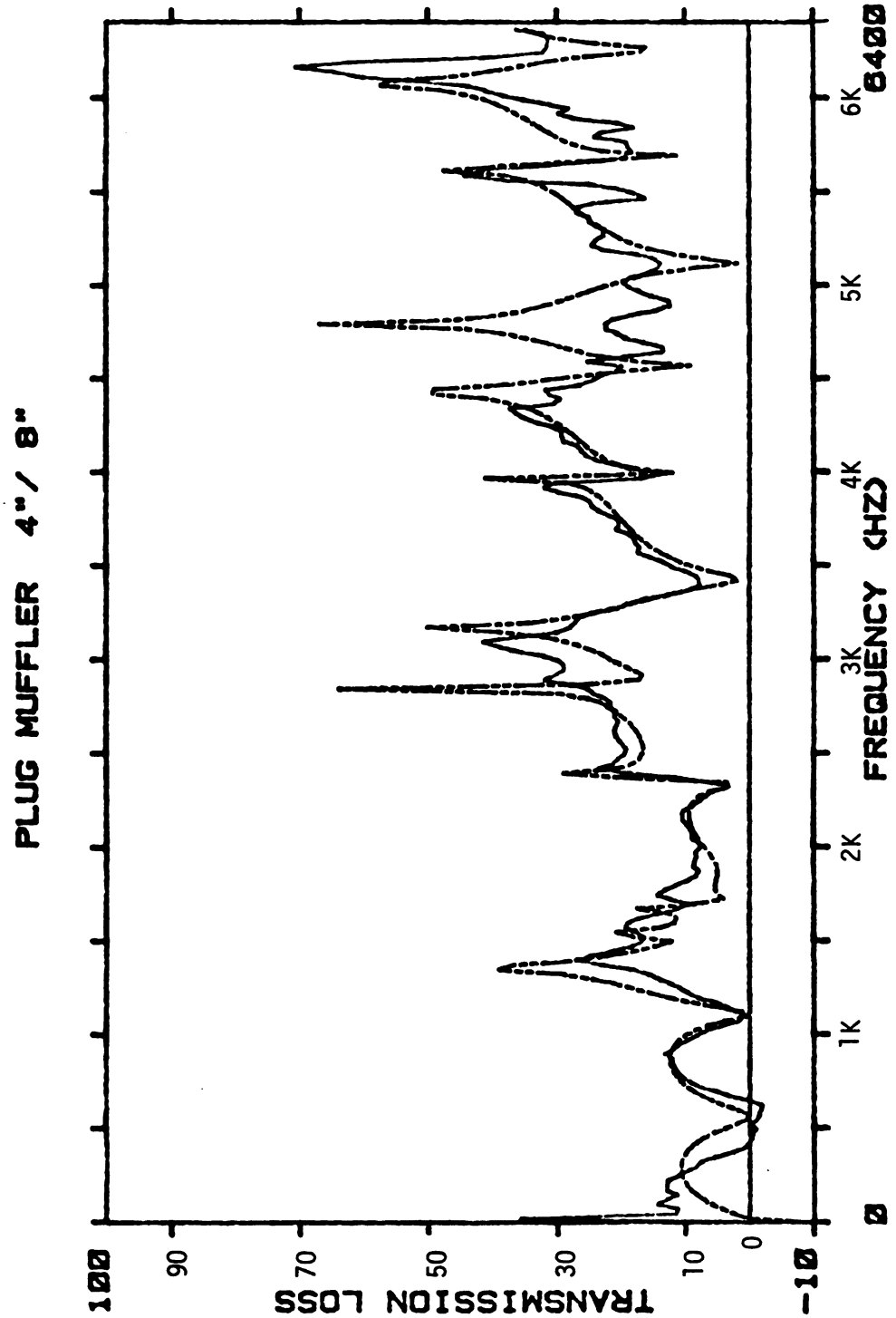

Figure 36. Plug muffler: ℓ_e = 4 in., ℓ_c = 8 in; $\sigma_e = \sigma_c$ = .049; M = 0.

——— experimental, ----- predicted.

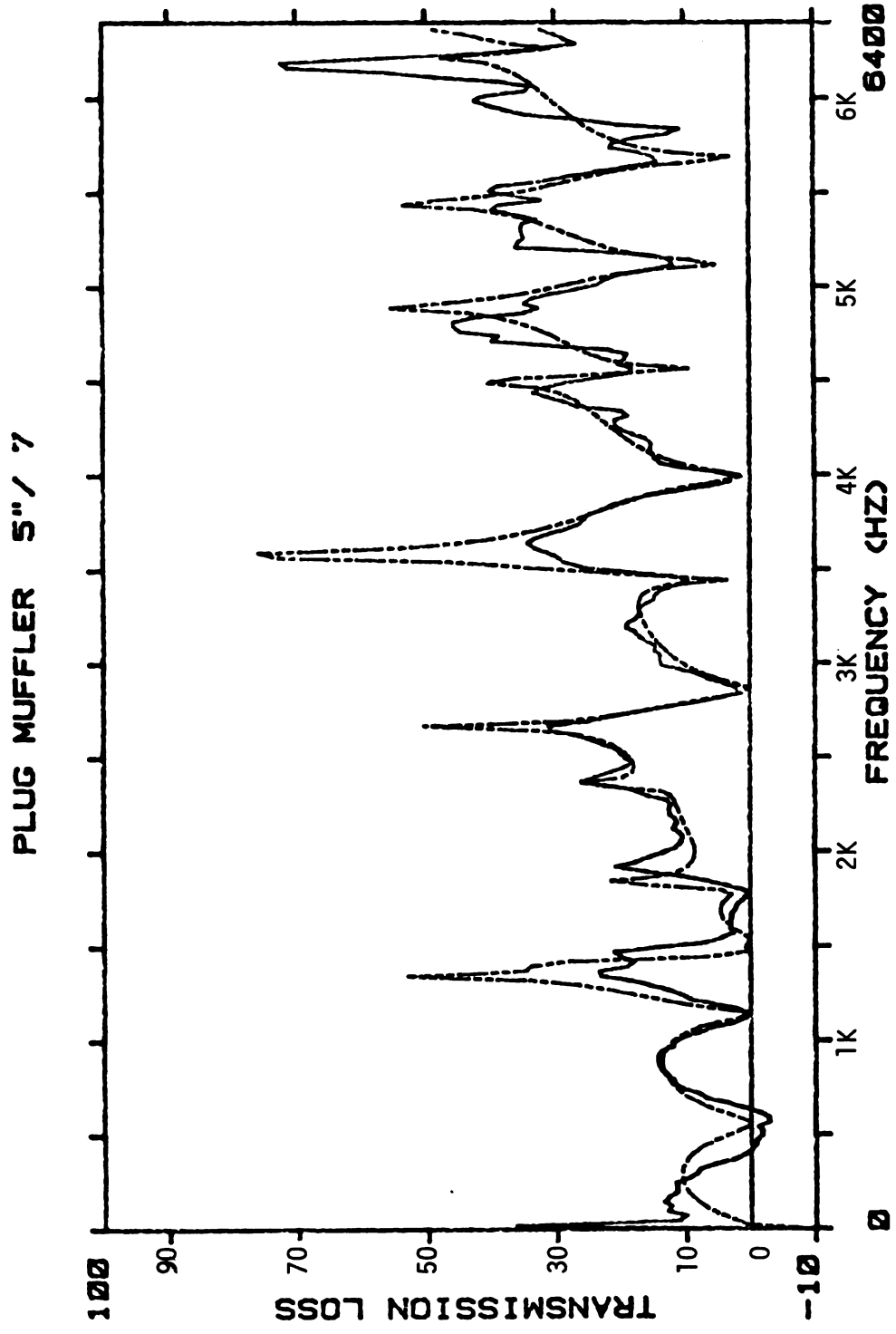

Figure 37. Plug muffler: ℓ_e = 5 in; ℓ_c = 7 in; $\sigma_e = \sigma_c$ = .049; M = 0.
—— experimental, ----- predicted

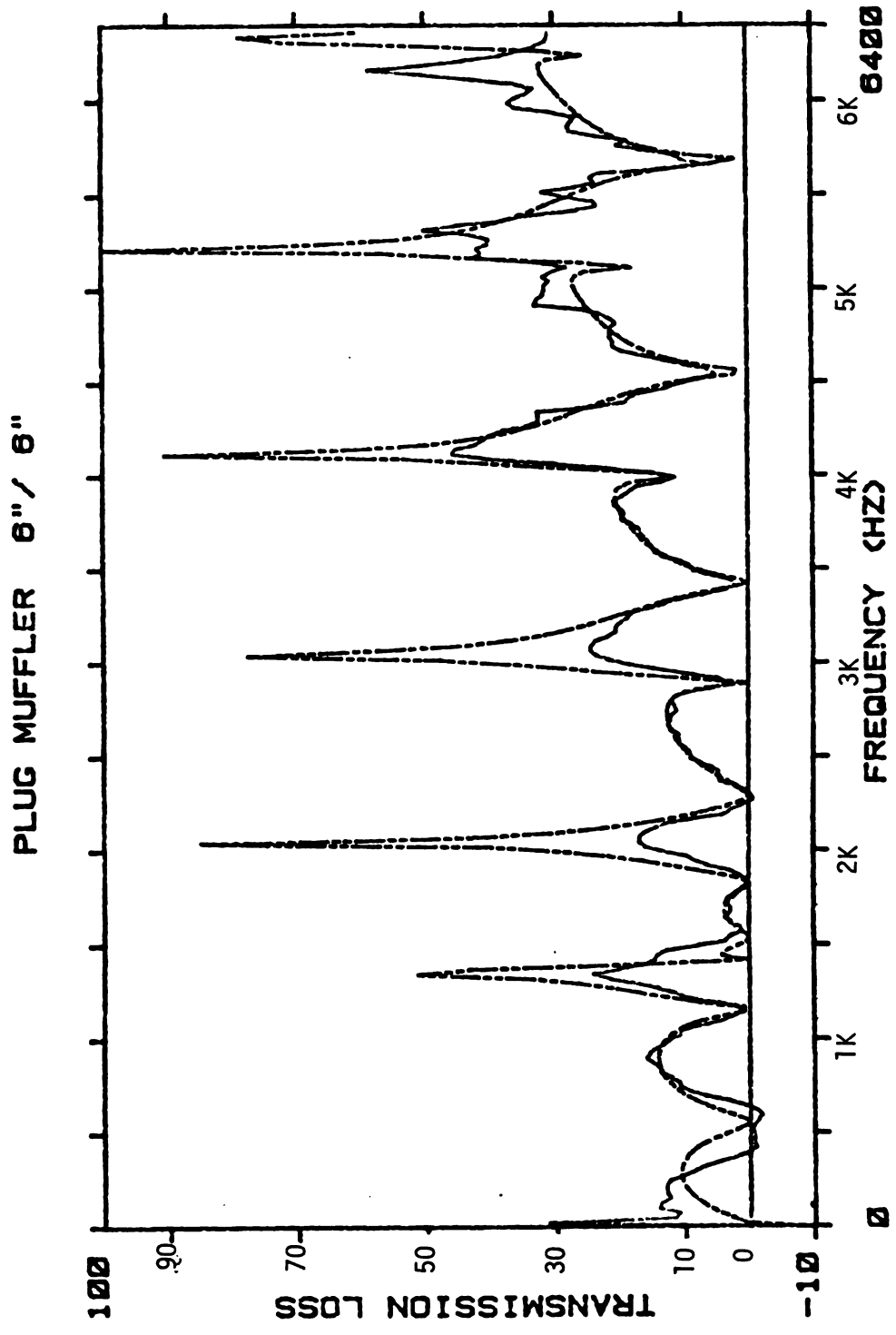

Figure 38. Plug muffler: $\ell_e = \ell_c = 6$ in, $\sigma_e = \sigma_c = .049$; M = 0.
——— experimental, ----- predicted